Integrators for highly oscillatory Hamiltonian systems: an homogenization approach

Claude Le Bris, Frédéric Legoll

INSTITUT NATIONAL DE RECHERCHE EN INFORMATIQUE ET EN AUTOMATIQUE

Integrators for highly oscillatory Hamiltonian systems: an homogenization approach

Claude Le Bris — Frédéric Legoll

N° ????

July 2007

Thème NUM

ISSN 0249-6399

Integrators for highly oscillatory Hamiltonian systems: an homogenization approach*

Claude Le Bris[†‡] , Frédéric Legoll[§‡]

Thème NUM — Systèmes numériques
Projet MICMAC

Rapport de recherche n° ???? — July 2007 — 53 pages

Abstract: We introduce a systematic way to construct symplectic schemes for the numerical integration of a large class of highly oscillatory Hamiltonian systems. The bottom line of our construction is to consider the Hamilton-Jacobi form of the Newton equations of motion, and to perform a two-scale expansion of the solution, for small times and high frequencies. The approximation obtained for the solution is then used as a generating function, from which the numerical scheme is derived. Several options for the derivation are presented, some of them also giving rise to non symplectic variants. The various integrators obtained are tested and compared to several existing algorithms. The numerical results demonstrate their efficiency.

Key-words: Numerical schemes, highly oscillatory Hamiltonian systems, generating function, two-scale expansion, symplectic algorithms.

* This work was supported by the Action Concertée Incitative "Nouvelles Interfaces des Mathématiques" SIMUMOL (Ministère de la Recherche et des Nouvelles Technologies, France) and by the INGEMOL non-thematic program (Agence Nationale de la Recherche). The authors thank Philippe Chartier for constant interaction and Ernst Hairer and Christian Lubich for stimulating discussions. The hospitality of the Isaac Newton Institute (Cambridge, UK) is gratefully acknowledged.

† CERMICS, Ecole Nationale des Ponts et Chaussées, 6 et 8 avenue Blaise Pascal, Cité Descartes, 77455 Marne-la-Vallée Cedex 2, France. Contact: lebris@cermics.enpc.fr

‡ INRIA Rocquencourt, MICMAC team-project, Domaine de Voluceau, B.P. 105, 78153 Le Chesnay Cedex, France.

§ LAMI, Ecole Nationale des Ponts et Chaussées, 6 et 8 avenue Blaise Pascal, Cité Descartes, 77455 Marne-la-Vallée Cedex 2, France. Contact: legoll@lami.enpc.fr

Unité de recherche INRIA Rocquencourt
Domaine de Voluceau, Rocquencourt, BP 105, 78153 Le Chesnay Cedex (France)
Téléphone : +33 1 39 63 55 11 — Télécopie : +33 1 39 63 53 30

Schémas numériques pour systèmes hamiltoniens hautement oscillants: une approche par l'homogénéisation

Résumé : Nous introduisons une méthode systématique permettant de construire des schémas symplectiques pour intégrer numériquement une grande classe de systèmes hamiltoniens hautement oscillants. L'idée principale est de considérer la formulation Hamilton-Jacobi des équations du mouvement, et de faire un développement à deux échelles de la solution, pour des temps petits et des fréquences élevées. On obtient ainsi une approximation de la solution de l'équation d'Hamilton-Jacobi, qui est ensuite utilisée comme fonction génératrice pour construire le schéma numérique. Plusieurs variantes sont présentées. Les différents schémas ainsi obtenus sont testés et comparés à plusieurs schémas existants. Les résultats numériques montrent leur efficacité.

Mots-clés : Schémas numériques, systèmes hamiltoniens hautement oscillants, fonction génératrice, développement à deux échelles, algorithmes symplectiques.

1 Introduction

This article presents a possible systematic methodology to design symplectic algorithms for a large class of highly oscillatory Hamiltonian dynamics. In short, our methodology consists in considering the Hamilton-Jacobi form of the Newton equations of motion, and performing a two-scale expansion of the solution, for small times and high frequencies. Some non-symplectic algorithms will also be introduced as variants of the symplectic ones.

The specific form of Hamiltonian systems we consider in this work writes

$$H_\varepsilon(q_1,q_2,p_1,p_2) = \frac{p_1^T p_1}{2} + \frac{p_2^T p_2}{2} + V_0(q_1,q_2) + (\Omega(q_1))^2 \, \frac{q_2^T q_2}{2\varepsilon^2}, \tag{1}$$

where $q = (q_1, q_2) \in \mathbb{R}^s \times \mathbb{R}^f$ and $p = (p_1, p_2) \in \mathbb{R}^s \times \mathbb{R}^f$ (the superscripts s and f respectively stand for the slow and the fast variables), and where V_0 is a potential energy that does not depend on ε. The important assumption in (1), which limits the applicability of our work, lies in the specific form of the Hamiltonian (1) as regards the fast degrees of freedom. It is assumed to be an *harmonic* oscillator

$$\frac{p_2^T p_2}{2} + (\Omega(q_1))^2 \, \frac{q_2^T q_2}{2\varepsilon^2} \quad \text{in those fast degrees of freedom.}$$

In addition, but this time this is not such a strong, structural assumption, we assume throughout this article that the fast frequency $\Omega(q_1)$ is a scalar quantity, and that there exists $c > 0$ such that $\Omega(q_1) \geq c > 0$ for all q_1. The case where $(\Omega(q_1))^2 \, \frac{q_2^T q_2}{2\varepsilon^2}$ is replaced by $\frac{q_2^T \Omega^2(q_1) q_2}{2\varepsilon^2}$, where $\Omega(q_1)$ is a $f \times f$ matrix, is, in principle, tractable with our approach, but leads to several technical difficulties that we have not been able to satisfactorily solve yet.

Our last assumption is that, for consistency, the initial conditions of the hamiltonian dynamics derived from (1) are assumed to only depend on ε in such a way that the system energy is bounded with respect to ε. In particular, this implies that q_2 is of order ε at initial time, a property that is propagated forward in time. We shall comment upon the above three assumptions below.

As is well-known, the numerical integration of the Newton equations derived from (1), namely

$$\frac{dq}{dt} = \frac{\partial H_\varepsilon}{\partial p}(q,p), \quad \frac{dp}{dt} = -\frac{\partial H_\varepsilon}{\partial q}(q,p), \tag{2}$$

using a standard symplectic scheme (such as velocity Verlet) is expensive. This originates from the smallness of ε, which dramatically reduces the size of admissible timesteps.

Our purpose is thus to design numerical integrators that are much more efficient. There already exist many works in this direction. Indeed, Hamiltonian systems of the type (1) have already been studied in the literature, see for instance [3, 4, 21]. In [21, Chap. XIII and XIV],

E. Hairer, Ch. Lubich and G. Wanner present in a unified way and analyze several algorithms designed for the integration of (2). A new algorithm, which also belongs to the class that is analyzed in [21], has been proposed in [15]. Another idea, following a WKB-type expansion of the solution of (2), is under study in [5]. We also mention the studies [10, 34], based on the Heterogeneous Multiscale Method paradigm, the Equilibrium method [24], and the methods proposed in [27, 29]. In contrast to the above works, and as announced above, our idea, in order to derive efficient algorithms for Hamiltonian systems which are symplectic *by construction*, is to work on the Hamilton-Jacobi form of the equations of motion. Otherwise stated, we adapt to the case of highly oscillatory systems the idea originally used by Feng in [12] to construct symplectic integrators. In fact, we will superimpose to the latter the idea of the two-scale expansion, natural in such a multiscale context.

Some important comments are already in order, both on our purpose and on the assumptions we make.

First, let us discuss in its own the purpose of constructing symplectic integrators for such multiscale Hamiltonian systems.

Certainly, symplectic schemes are natural for the integration of Hamiltonian systems since they reproduce at the discrete level an important geometric property of the exact flow. More than natural, symplectic schemes are also proved to be efficient as regards the conservation of the energy and of the possible invariants of the system over extremely long times (see [21, Chap. IX and X] and [1, 18, 31]; see also [17] where, on a numerical example, symplectic methods are shown to be superior to some non-symplectic methods that exactly preserve the energy). The proof of this property, as is well-known, relies on backward error analysis (along, for the conservation of the invariants, with some elements of KAM theory). In any case, the properties of conservation are obtained in the limit of small time steps. This is where our context of highly oscillatory equations somehow collides with the above line of thought. For backward error analysis to hold true, the timestep has to be small compared to ε (the shortest period present in the system), but, for efficiency, the timestep used in practice needs to be much larger than ε. So, we will not be able to invoque backward error analysis to justify the long time conservation properties of the scheme. The notion of symplecticity in its own may even be considered of poor interest in this particular context (see the introduction of Chapter XIII of [21]). Ideally, what we would need is a notion of *partial symplecticity* with respect to the slow degrees of freedom in the system. In the absence of such a notion, and of the corresponding construction, the best we can do is construct a "globally" symplectic scheme, and *observe* its actual conservation properties.

Another property that could be of interest, alternatively to symplecticity, is *symmetry*. One of the schemes we construct below is symmetric, the others are not. At present time, it is not clear, to us at least, how symmetry is related to long time conservation properties. The literature does not seem to provide a definite understanding of this issue: examples [19] and counterexamples [11] exist, showing the complexity of the situation. Despite such a growing literature, the understanding of symmetric methods is not at the level of that of symplectic methods. In addition, symmetric schemes are often implicit, and we will try to

avoid as much as possible implicitness. We will nevertheless come back to symmetry, when we address numerical analysis later in this introduction.

A last general point we would like to emphasize, before getting to some other types of comments, is that we are after the computations of *trajectories*. Our purpose here is *not* to construct a reduced system, involving only the slow degrees of freedom in the presence of some effective potential created by the (eliminated) fast degrees of freedom. We do not want either to directly compute averages based on the trajectories. For both above issues, there are a lot of relevant, excellent, studies and approaches in the literature. The only question we examine here is: are we able, while keeping all the degrees of freedom explicit, to approximate as accurately as possible the trajectories over long times?

Second, let us briefly comment upon our assumptions. There are three of them: the form of the Hamiltonian, the form of the fast frequency $\Omega(q_1)$, the size of the initial conditions.

Our approach applies to Hamiltonians that are *harmonic in the fast variables*. Although this specific form is quite general, and already used in the literature, we conceed that this is a strict, structural, limitation of our work. This is related to our technique of derivation. The harmonicity of the Hamiltonian with respect to the fast degrees of freedom translates into the (partial) periodicity of the generating function S_ε, a property that is subsequently used to close the hierarchy of equations produced by the two-scale expansion (see Section 2.1). Somehow, this harmonicity hypothesis *assumes* that some preliminary work has been performed on the original Hamiltonian in order to approximate its fast degrees of freedom. It is not *a priori* impossible that some analogous derivation could be performed for slightly more general Hamiltonian. In homogenization theory, it is indeed well-known that periodicity is an assumption that may be relaxed in various directions (think of *stochastic* homogenization, etc.). However, it is unlikely that *all* Hamiltonians will be tractable with such an approach. This has the following consequence: in order to compare the integrators we derive with other, more generic integrators (such as the Impulse method [16, 35] or the Mollify method [13, 33]) in a fair manner, we will bear in mind the specificity of our setting.

A case more general than (1) would be to consider the Hamiltonian

$$H_\varepsilon(q,p) = \frac{p^T p}{2} + V_0(q) + \frac{1}{\varepsilon^2} V_{\text{fast}}(q), \tag{3}$$

where V_0 and V_{fast} do not depend on ε, and where there exists a global change of variable $q \mapsto Q = \chi(q)$ such that $V_{\text{fast}}(\chi^{-1}(Q)) = \frac{1}{2} Q_2^T A(Q_1) Q_2$ for some (say positive definite) matrix $A(Q_1)$. In other words, the fast energy is indeed harmonic, but *not* in the original cartesian coordinates. We recover the case (1) when the map χ is simply the identity map. This form of Hamiltonian (with a fast energy that is harmonic up to a change of variable) is very frequent *e.g.* in molecular dynamics. Because we keep the harmonicity assumption, there is some hope we can handle such cases within our approach. However, in practice, the map χ is difficult to manipulate, so an approach based on rewriting the problem in the Q variable seems poorly interesting.

Our second assumption concerns the fast frequency $\Omega(q_1)$. The expression (1) shows a *scalar* $\Omega(q_1)$. This is the only case we shall consider in this article. In other words, this corresponds to a spherical matrix of frequencies, and to fixed eigenmodes that all share the same eigenvalue. There are several extensions of this simple case. First, the fast frequency can be a constant, non spherical matrix. The exponential algorithms described in [21, Chap. XIII] can handle this case. Second, the fast frequency $\Omega(q_1)$ can be a non-constant diagonal matrix. This corresponds to the case when the eigenvalues depend on q_1, but the eigenmodes are fixed. A third case corresponds to a matrix-valued fast frequency $\Omega(q_1)$ for which *both* eigenvalues and eigenmodes vary as q_1 changes. This case is much more complicated than the previous ones. Some algorithms are proposed in [21, Chap. XVI] (see also [25, 26, 30], and [23] for a different approach). They require the diagonalization of the matrix $\Omega(q_1)$ at each macroscopic time step, which is of course expensive. However, no other solution seems possible to date. In particular, the idea to use an algorithm that has been designed in the case of a constant frequency matrix Ω, with the current value $\Omega(q_1)$ of the frequency (considered fixed over a macroscopic time-step) does not seem to lead to efficient algorithms. A fourth case is when, in addition to varying eigenvalues and eigenmodes, some fast eigenvalues cross each other. This leads to the apparition of a third time scale (in addition to the slow and the fast ones), which is the characteristic time of level crossing. An illustrative and simple example can be seen in [21, p 535]. The state-of-the-art approach on this case consists in adapting the time step, so as to decrease it when eigenvalue crossings are about to occur. The interested reader will find a short review on these different cases in [8]. Clearly, the scalar case that we consider here is rather simple in comparison to the ones we have mentioned. However, it is rich enough to allow for several interesting variants of our construction.

As regards initial conditions, we have chosen to work with initial conditions whose energy is bounded, uniformly in ε. We have mentioned that this implies that the position of the fast variable, q_2, is indeed also bounded from above by ε. Therefore, the nonlinear feedback it might have on the slow degrees of freedom, *via* the potential $V_0(q_1, q_2)$, is all the smaller. When testing the integrators, we will thus take care of testing them over an extremely long time frame, so as to let the possible instabilities develop.

Finally, and in addition to this list of comments, let us emphasize one, extremely important mathematical point, not to say weakness, in our derivation. We are unable to perform any numerical analysis of our algorithms. This would clearly provide a rigourous understanding. We are only in position to test the integrators numerically, and observe their remarkable efficiency. Actually, to the best of our knowledge, it seems that the only numerical analysis tool that is available in the context of highly oscillatory Hamiltonian systems is the Modulated Fourier Expansion (MFE) (see [21, Sec. XIII.5], [6, 7, 20]), which currently works well to analyze certain symmetric schemes. So, although symmetric schemes are often implicit (such as Algorithm 2.6 that we propose in Section 2.3), they are interesting because they *may* allow for a numerical analysis.

The plan of our work is as follows. We will first consider the case when the fast frequency is constant. Section 2 describes the derivation of several algorithms and Section 3 shows the numerical results on some commonly used test case. Next, in Section 4, we address the case when the fast frequency actually depends on the slow position q_1. We hope to be able to return in future publications to the other, more complicated cases, of fast frequencies. Note that the methodology described here in details has been introduced in [28]. We also outlined there the derivation of *some* (but not all) algorithms presented below. Even in the present *extended and updated* version, it is not possible to give all the details of the calculations, which might be rather tedious, although not difficult. We have thus chosen to postpone to two appendices some calculations. Some other details are simply omitted, for brevity.

We conclude this introduction by some preliminary calculations, which will in particular make the above strategy somewhat more precise.

Let $\overline{S}_\varepsilon(t,q,P)$ be the solution of

$$\partial_t \overline{S}_\varepsilon = H_\varepsilon\left(q + \partial_P \overline{S}_\varepsilon, P\right), \quad \overline{S}_\varepsilon(0,q,P) = 0. \tag{4}$$

For all (q,p,t), we know that $(Q(t),P(t))$, implicitly defined by

$$p = P(t) + \frac{\partial \overline{S}_\varepsilon}{\partial q}(t,q,P(t)), \quad Q(t) = q + \frac{\partial \overline{S}_\varepsilon}{\partial P}(t,q,P(t)), \tag{5}$$

solve (2) with the initial conditions (q,p).

It is well-known that several sets of variables may be employed to write the Hamilton-Jacobi equation. Let us briefly motivate our choice, namely (q,P). First, the choice (q,Q) is not convenient because the generating function in these variables is singular in the limit $t \to 0$. This is of course prohibitive for our purpose, where we intend to use a Taylor expansion of $\overline{S}_\varepsilon$ for *small* times t. Another possible choice is (Q,p). This actually leads to algorithms with the same properties as those derived here with (q,P). In addition, it is also possible to choose the variables in such a way that the resulting algorithm is symmetric (and often implicit). In the present article, we work with the variables (q,P), and derive several explicit non-symmetric algorithms (see Algorithms 2.1, 2.2, 2.3 and 2.4 in Sections 2.1 and 2.2 below, and Algorithm 4.1 in Section 4.1) and one implicit symmetric algorithm (see Algorithm 2.6 in Section 2.3).

At this stage, we are in position to more explicitly describe our approach. Using a two-scale type Ansatz, we derive an approximation of the solution $\overline{S}_\varepsilon(h,q,P)$ of (4) at time $t = h$, for a small parameter ε and for a time step h which is small yet much larger than ε (hence the computational efficiency). Once obtained, this approximation is inserted in the change of variables (5) and a symplectic integrator for (1)-(2) follows. Slightly modifying the above lines, we are also able to derive schemes, which although not necessarily symplectic, will outperform all existing integrators when used on the particular context of Hamiltonians (1).

Before we proceed, we need to make a slight preparation. As we have already noticed, the variable q_2 is of order ε, because the energy is bounded. It is thus appropriate to proceed

with a change of variable and of unknown function in (4). We set

$$r_2 = \frac{\Omega(q_1)}{\varepsilon} q_2 \quad \text{and} \quad S_\varepsilon(t, q_1, r_2, P_1, P_2) = \overline{S}_\varepsilon \left(t, q_1, \frac{\varepsilon r_2}{\Omega(q_1)}, P_1, P_2 \right).$$

It follows that, in this new set of variables, S_ε satisfies

$$\begin{aligned} \partial_t S_\varepsilon &= \frac{P_1^T P_1}{2} + \frac{P_2^T P_2}{2} + V_0 \left(q_1 + \partial_{P_1} S_\varepsilon, \frac{\varepsilon r_2}{\Omega(q_1)} + \partial_{P_2} S_\varepsilon \right) \\ &+ \frac{1}{2} \left(\frac{\Omega(q_1 + \partial_{P_1} S_\varepsilon)}{\varepsilon} \right)^2 \left(\frac{\varepsilon r_2}{\Omega(q_1)} + \partial_{P_2} S_\varepsilon \right)^2 \end{aligned} \tag{6}$$

with the initial condition

$$\forall q_1, \ \forall r_2, \ \forall P_1, \ \forall P_2, \quad S_\varepsilon(0, q_1, r_2, P_1, P_2) = 0. \tag{7}$$

This is the form we will use in the sequel.

2 The case of a constant fast frequency

In this section, we consider the case when $\Omega(q_1) \equiv \Omega$ does not depend on q_1. We make the Ansatz

$$\begin{aligned} S_\varepsilon(t, q_1, r_2, P_1, P_2) &= S_0(t, \tau, q_1, r_2, P_1, P_2) + \varepsilon S_1(t, \tau, q_1, r_2, P_1, P_2) \\ &+ \text{higher order terms in } \varepsilon^k, \ k \geq 2, \end{aligned} \tag{8}$$

where the fast time τ is

$$\tau = \frac{t\Omega}{\varepsilon}, \tag{9}$$

and where the functions $(S_k)_{k \geq 0}$ are supposed to be 2π periodic in τ.

In order to motivate this Ansatz, let us consider the case when V_0 does not depend on q_2. Fast and slow variables are then decoupled and the solution to (6)-(7) reads

$$S_\varepsilon = S_{\text{slow}}(t, q_1, P_1) + \varepsilon \tilde{S}(\tau, r_2, P_2),$$

where τ is defined by (9), $S_{\text{slow}}(t, q_1, P_1)$ solves the Hamilton-Jacobi equation

$$\partial_t S_{\text{slow}} = H_1(q_1 + \partial_{P_1} S_{\text{slow}}, P_1), \quad S_{\text{slow}}(0, q_1, P_1) = 0 \tag{10}$$

associated to the Hamiltonian $H_1 = \dfrac{p_1^T p_1}{2} + V_0(q_1)$, and

$$\tilde{S}(t, r_2, P_2) = \frac{1}{\Omega} \left[\left(\frac{P_2^T P_2 + r_2^T r_2}{2} \right) \tan \tau + P_2^T r_2 \left(\frac{1}{\cos \tau} - 1 \right) \right]$$

is indeed 2π periodic in τ. So, in this simple case, the exact solution to (6)-(7) is consistent with our Ansatz (8).

In the case under consideration of a constant fast frequency, we will present three variants of our strategy. A natural idea consists in applying our approach directly on Eq. (6), that is in the original coordinates (q_1, q_2, p_1, p_2). We follow this idea in Section 2.1. In view of the schemes obtained there, it is tempting to introduce a modified scheme, still in the variables (q_1, q_2, p_1, p_2), which is not symplectic (because not derived from a generating function), but happens to be very efficient (see Section 2.2). A third idea is to first perform a change of variables, so as to analytically integrate the fast motion, and to only apply our approach in a second stage (see Section 2.3). In the three cases, we obtain efficient algorithms. The present section is dedicated to the design of all these algorithms. We report on their numerical performances in Section 3.

2.1 Derivation of symplectic schemes

We now insert our Ansatz (8) in (6)-(7) and expand in powers of ε. From the initial condition (7), we obtain

$$\forall k \geq 0, \quad S_k(t=0, \tau=0, q_1, r_2, P_1, P_2) = 0. \tag{11}$$

The equations of order ε^{-2} and ε^{-1} respectively read

$$\frac{\partial S_0}{\partial P_2} = 0 \quad \text{and} \quad \frac{\partial S_0}{\partial \tau} = 0. \tag{12}$$

The equation of order ε^0 reads

$$\partial_t S_0 + \Omega \partial_\tau S_1 = \frac{P_1^T P_1}{2} + \frac{P_2^T P_2}{2} + V_0(q_1 + \partial_{P_1} S_0, 0) + \frac{1}{2}\left(r_2 + \Omega \partial_{P_2} S_1\right)^2, \tag{13}$$

whereas the equation of order ε reads

$$\partial_t S_1 + \Omega \partial_\tau S_2 = \Omega (r_2 + \Omega \partial_{P_2} S_1)^T \partial_{P_2} S_2 + (\nabla_1 V_0)^T \partial_{P_1} S_1 + \frac{1}{\Omega} (\nabla_2 V_0)^T \left(r_2 + \Omega \partial_{P_2} S_1\right), \tag{14}$$

where all derivatives of V_0 are evaluated at $(q_1 + \partial_{P_1} S_0, 0)$.

Our aim is now to use (13) and the periodicity of S_1 in τ in order to get a closed equation on S_0. Without a further approximation, it is however impossible at this stage, for a reason that is made clear in Remark 1. Following Feng [12], we thus perform an expansion with respect to the variable t, for $t > 0$ small. More precisely, we further expand (13) and (14) in powers of t, and obtain an equation for each power of ε and t.

The equation of order $\varepsilon^0 t^0$ reads

$$\partial_t S_0(t=0) + \Omega \partial_\tau S_1(t=0) = \frac{P_1^T P_1}{2} + \frac{P_2^T P_2}{2} + V_0(q_1, 0) + \frac{1}{2}\left(r_2 + \Omega \partial_{P_2} S_1(t=0)\right)^2. \tag{15}$$

Let us introduce

$$\begin{aligned} A(\tau, q_1, r_2, P_1, P_2) &= \Omega S_1(t=0, \tau, q_1, r_2, P_1, P_2) \\ &- \tau \left(\frac{P_1^T P_1}{2} + V_0(q_1, 0) - \partial_t S_0(t=0, q_1, r_2, P_1) \right). \end{aligned} \tag{16}$$

The function S_0 does not depend on τ and P_2 (see (12)). So, the function A satisfies $A(\tau = 0, q_1, r_2, P_1, P_2) = 0$ and

$$\partial_\tau A = \frac{P_2^T P_2}{2} + \frac{1}{2} \left(r_2 + \frac{\partial A}{\partial P_2} \right)^2. \tag{17}$$

For any given q_1 and P_1, we recognize the Hamilton-Jacobi equation in variables (τ, r_2, P_2) associated to the harmonic oscillator of energy $(r_2^T r_2 + p_2^T p_2)/2$. The analytical expression of such a generating function is known, and reads

$$A = \left(\frac{P_2^T P_2 + r_2^T r_2}{2} \right) \tan\tau + P_2^T r_2 \left(\frac{1}{\cos\tau} - 1 \right). \tag{18}$$

Equation (18) shows that A is 2π periodic in τ. Inserting this in (16), and recalling that S_1 is also 2π periodic in τ, we obtain

$$\partial_t S_0(t=0) = \frac{P_1^T P_1}{2} + V_0(q_1, 0), \tag{19}$$

$$S_1(t=0) = \frac{1}{\Omega} \left(\frac{P_2^T P_2 + r_2^T r_2}{2} \right) \tan\tau + \frac{P_2^T r_2}{\Omega} \left(\frac{1}{\cos\tau} - 1 \right), \tag{20}$$

where $\partial_t S_0$ and S_1 are both evaluated at $(t = 0, \tau, q_1, r_2, P_1, P_2)$. Note that, in view of (11) and (12), we have that $S_0(t=0) = 0$.

There is no major difficulty in the sequel of the identification procedure. We thus refer the reader to Appendix 5 for the details. The equations obtained are the following:

$$\frac{\partial^2 S_0}{\partial t^2}(t=0) = P_1^T \nabla_1 V_0(q_1, 0), \tag{21}$$

$$\frac{\partial^3 S_0}{\partial t^3}(t=0) = (\nabla_1 V_0(q_1, 0))^T \nabla_1 V_0(q_1, 0) + P_1^T \nabla_{11} V_0(q_1, 0) P_1, \tag{22}$$

$$\partial_t S_1(t=0) = \partial_{tt} S_1(t=0) = 0, \tag{23}$$

$$S_2(t=0) = \frac{1}{\Omega^2} (\nabla_2 V_0(q_1, 0))^T \left(\frac{P_2}{\cos\tau} - P_2 + (\tan\tau) r_2 \right), \tag{24}$$

$$\begin{aligned} \partial_t S_2(t=0) &= \frac{-1}{2\Omega^2} (\nabla_2 V_0(q_1, 0))^T \nabla_2 V_0(q_1, 0) - \frac{1}{\Omega^2} P_1^T \nabla_{12} V_0(q_1, 0) P_2 \\ &+ \frac{1}{4\Omega^2 \cos^2\tau} \left(P_2^T \nabla_{22} V_0 P_2 + r_2^T \nabla_{22} V_0 r_2 + 2 \sin\tau r_2^T \nabla_{22} V_0 P_2 \right). \end{aligned} \tag{25}$$

All the functions S_k and their derivatives are evaluated at $(t=0,\tau,q_1,r_2,P_1,P_2)$, while V_0 and its derivatives are evaluated at $(q_1,0)$. The equation (22) is derived in Appendix 5.3. In a similar way, we obtain the expression for $\dfrac{\partial^4 S_0}{\partial t^4}(t=0)$, which only depends on q_1 and P_1.

Remark 1 *With S_0 and S_1 solutions of (13), we can introduce*

$$\begin{aligned} A(t,\tau,q_1,r_2,P_1,P_2) &= \Omega S_1(t,\tau,q_1,r_2,P_1,P_2) \\ &- \tau\left(\frac{P_1^T P_1}{2} + V_0(q_1+\partial_{P_1}S_0,0) - S_0(t,q_1,r_2,P_1)\right), \end{aligned}$$

which satisfies (17). So, for each t, q_1 and P_1, we recognize the Hamilton-Jacobi equation in the variables (τ,r_2,P_2) associated to the harmonic oscillator $(r_2^T r_2 + p_2^T p_2)/2$. However, we only know the initial condition for A (at $\tau=0$) for the very specific value $t=0$, and not for the other values $t\neq 0$. Expanding (13) in powers of t, as we did above, is a way to circumvent this difficulty.

Considering (21)-(25), we decide to approximate $S_\varepsilon(h)$ by

$$\boxed{\widetilde{S_\varepsilon}(h) := S_0 + h\partial_t S_0 + \frac{h^2}{2}\partial_{tt}S_0 + \varepsilon S_1 + \varepsilon^2 S_2 + \varepsilon^2 h\partial_t S_2,} \tag{26}$$

where all the functions S_k and their derivatives are evaluated at $(t=0,\tau,q_1,r_2,P_1,P_2)$. We now motivate the choice (26) and the truncations that we decide to make in the series in powers of ε and h. First, numerical tests we performed show that we need to take into account the high-order term $\partial_t S_2$ in the approximation. This will be further explained in Remark 6 below. Let us here study the error between $S_\varepsilon(h)$ and its approximation (26) and how this error propagates to the scheme. We have

$$\begin{aligned} S_\varepsilon(h,q_1,r_2,P_2,P_1) &= S_0(h,q_1,r_2,P_1) + \varepsilon S_1(h,\tau,q_1,r_2,P_2,P_1) \\ &\quad +\varepsilon^2 S_2(h,\tau,q_1,r_2,P_2,P_1) + \varepsilon^3 e_3(\varepsilon,h,q_1,r_2,P_1,P_2), \\ S_0(h,q_1,r_2,P_1) &= S_0 + h\partial_t S_0 + \frac{h^2}{2}\partial_{tt}S_0 + \frac{h^3}{6}\frac{\partial^3 S_0}{\partial t^3} + \frac{h^4}{24}\frac{\partial^4 S_0}{\partial t^4} \\ &\quad +h^5 e_0(h,q_1,r_2,P_1), \\ S_1(h,\tau,q_1,r_2,P_2,P_1) &= S_1 + h\partial_t S_1 + \frac{h^2}{2}\partial_{tt}S_1 + h^3 e_1(h,\tau,q_1,r_2,P_1,P_2), \\ S_2(h,\tau,q_1,r_2,P_2,P_1) &= S_2 + h\partial_t S_2 + h^2 e_2(h,\tau,q_1,r_2,P_1,P_2), \end{aligned}$$

with $\tau = \Omega h/\varepsilon$, for some error functions e_0, e_1, e_2 and e_3 which are smooth functions of their arguments. Hence, we obtain

$$S_\varepsilon(h) = \widetilde{S_\varepsilon}(h) + E^\varepsilon(h,q_1,r_2,P_1,P_2)$$

with

$$\begin{aligned} E^\varepsilon(h,q_1,r_2,P_1,P_2) &= \frac{h^3}{6}\frac{\partial^3 S_0}{\partial t^3}(q_1,P_1)+\frac{h^4}{24}\frac{\partial^4 S_0}{\partial t^4}(q_1,P_1)+h^5 e_0(h,q_1,r_2,P_1) \\ &+ \varepsilon h^3 e_1(h,\tau,q_1,r_2,P_1,P_2)+\varepsilon^2 h^2 e_2(h,\tau,q_1,r_2,P_1,P_2) \\ &+ \varepsilon^3 e_3(\varepsilon,h,q_1,r_2,P_1,P_2). \end{aligned}$$

There is no remainder of order εh and εh^2 in view of (23), and recall that $\dfrac{\partial^3 S_0}{\partial t^3}$ and $\dfrac{\partial^4 S_0}{\partial t^4}$ do not depend on r_2 and P_2. In view of (5), we have

$$Q_2 = q_2 + \frac{\partial S_\varepsilon(h)}{\partial P_2} = q_2 + \frac{\partial \widetilde{S_\varepsilon}(h)}{\partial P_2} + \frac{\partial R^\varepsilon}{\partial P_2}.$$

We see that $\dfrac{\partial \widetilde{S_\varepsilon}(h)}{\partial P_2}$ is a sum of three terms of respective order ε, ε^2 and $\varepsilon^2 h$, whereas $\dfrac{\partial R^\varepsilon}{\partial P_2}$ is a sum of four terms of respective order h^5, εh^3, $\varepsilon^2 h^2$ and ε^3. We now work in the regime

$$\varepsilon \ll h \ll \sqrt{\varepsilon}. \tag{27}$$

Notice that other choices of regime are possible. Then, the four terms of $\dfrac{\partial R^\varepsilon}{\partial P_2}$ are negligible compared to any of the three terms of $\dfrac{\partial \widetilde{S_\varepsilon}(h)}{\partial P_2}$. The same holds true for the equation that defines P_2. For the slow position, we have

$$Q_1 = q_1 + \frac{\partial \widetilde{S_\varepsilon}(h)}{\partial P_1} + \frac{\partial R^\varepsilon}{\partial P_1}.$$

The quantity $\dfrac{\partial R^\varepsilon}{\partial P_1}$ includes a term of order h^3, which is not negligible compared to the term of order $\varepsilon^2 h$ which appears in $\dfrac{\partial \widetilde{S_\varepsilon}(h)}{\partial P_1}$. However, since we keep all the terms that come from $\widetilde{S_\varepsilon}(h)$ for the fast variables, we also need to keep all of them for the slow variables, in order for the scheme to be symplectic. To conclude on this point, we have thus checked that the choice (26) is consistent with the regime (27).

When inserted in (5), the approximation (26) provides a symplectic scheme. In view of (5),

$$\boxed{p = P_h + \frac{\partial \widetilde{S_\varepsilon}(h)}{\partial q}(q,P_h), \quad Q_h = q + \frac{\partial \widetilde{S_\varepsilon}(h)}{\partial P}(q,P_h)} \tag{28}$$

defines a symplectic map $\widetilde{\Psi}_h : (q,p) \mapsto (Q_h,P_h)$. The corresponding scheme reads $(q_{n+1},p_{n+1}) = \widetilde{\Psi}_h(q_n,p_n)$. The scheme is unfortunately ill-defined for some values of τ. Indeed, in view of

(28), the equation for P_2 (the fast component of P_h) reads

$$p_2 = P_2 + \frac{\partial \widetilde{S_\varepsilon}(h)}{\partial q_2} = P_2 + \frac{\Omega}{\varepsilon}\frac{\partial \widetilde{S_\varepsilon}(h)}{\partial r_2}, \tag{29}$$

which yields

$$\left(\mathrm{Id}_f + \frac{\varepsilon h \tan\tau}{2\Omega}\nabla_{22}V_0(q_1,0)\right) P_2 = \\ (\cos\tau)p_2 - (\sin\tau)r_2 - \frac{\varepsilon}{\Omega}\sin\tau\nabla_2 V_0(q_1,0) - \frac{\varepsilon h}{2\Omega\cos\tau}\nabla_{22}V_0(q_1,0)r_2,$$

with $\tau = \Omega h/\varepsilon$ and $r_2 = \Omega q_2/\varepsilon$, and where Id_f is the identity matrix of size $f \times f$. If $\mathrm{Id}_f + \frac{\varepsilon h \tan\tau}{2\Omega}\nabla_{22}V_0(q_1,0) = 0$, then P_2 is not defined. Note that this difficulty may arise even if V_0 does not depend on q_1 (in that case, the slow and fast variables are not coupled).

In order to circumvent this difficulty, we are going to slightly modify the expansion (26). For this purpose, let us momentarily keep (26), insert it in (5), obtain (29) which more explicitly reads

$$p_2 = P_2 + \frac{\partial}{\partial r_2}\left[\Omega S_1(t=0) + \varepsilon\Omega S_2(t=0) + \varepsilon h\Omega\partial_t S_2(t=0)\right].$$

Using (20), (24) and (25), we next obtain

$$\begin{aligned}
\Omega S_1(t=0) \;+\; & \varepsilon\Omega S_2(t=0) + \varepsilon h\Omega\partial_t S_2(t=0) \\
= \;& \left(\frac{P_2^T P_2 + r_2^T r_2}{2}\right)\tan\tau + P_2^T r_2\left(\frac{1}{\cos\tau} - 1\right) \\
+ \;& \frac{\varepsilon}{\Omega}\left(\nabla_2 V_0(q_1,0)\right)^T\left(\frac{P_2}{\cos\tau} - P_2 + (\tan\tau)r_2\right) \\
- \;& \frac{\varepsilon h}{2\Omega}(\nabla_2 V_0(q_1,0))^2 - \frac{\varepsilon h}{\Omega}P_1^T\nabla_{12}V_0(q_1,0)P_2 \\
+ \;& \frac{\varepsilon h}{4\Omega\cos^2\tau}\left(P_2^T\nabla_{22}V_0P_2 + r_2^T\nabla_{22}V_0 r_2 + 2\sin\tau r_2^T\nabla_{22}V_0P_2\right).
\end{aligned}$$

The right-hand side may now be rearranged. The term quadratic in P_2 reads $\frac{1}{2}P_2^T M P_2$, where

$$\begin{aligned}
M = \tan(\tau\mathrm{Id}_f) + \frac{\varepsilon h}{2\Omega\cos^2\tau}\nabla_{22}V_0 \;&=\; \tan\left(\tau\mathrm{Id}_f + \frac{\varepsilon h}{2\Omega}\nabla_{22}V_0\right) + O(\varepsilon^2h^2) \\
&=\; \tan\left(h\frac{\Omega}{\varepsilon}\mathrm{Id}_f + \frac{\varepsilon h}{2\Omega}\nabla_{22}V_0\right) + O(\varepsilon^2h^2).
\end{aligned}$$

It is thus natural to introduce the matrix

$$\Omega_\varepsilon(q_1) = \frac{\Omega}{\varepsilon}\,\mathrm{Id}_f + \frac{\varepsilon}{2\Omega}\nabla_{22}V_0(q_1,0), \tag{30}$$

the new variables

$$\overline{q}_2 = q_2 + \frac{\varepsilon^2}{\Omega^2}\nabla_2 V_0(q_1,0), \quad \overline{P}_1 = P_1 - \frac{\varepsilon^2}{\Omega^2}\nabla_{12}V_0(q_1,0)P_2, \tag{31}$$

and replace (26) by

$$\boxed{\begin{array}{rcl} S_\varepsilon^{\mathrm{symp1}}(h) & := & h\left[V_0(q_1,0) - \dfrac{\varepsilon^2}{2\Omega^2}\left(\nabla_2 V_0(q_1,0)\right)^T\nabla_2 V_0(q_1,0) + \dfrac{1}{2}\overline{P}_1^T\overline{P}_1\right] \\ & & +\dfrac{h^2}{2}(\nabla_1 V_0(q_1,0))^T\overline{P}_1 \\ & + & \dfrac{1}{2}P_2^T\Omega_\varepsilon^{-1}(q_1)\tan(h\Omega_\varepsilon(q_1))\,P_2 + \dfrac{1}{2}\overline{q}_2^T\Omega_\varepsilon(q_1)\tan(h\Omega_\varepsilon(q_1))\,\overline{q}_2 \\ & & +P_2^T(\cos^{-1}(h\Omega_\varepsilon(q_1)) - \mathrm{Id}_f)\,\overline{q}_2. \end{array}} \tag{32}$$

The difference between (32) and (26) is of order $O(\varepsilon^3) + O(\varepsilon^2 h^2)$, so the order of the approximation has not been modified. The motivation for introducing $\overline{q}_2$ is that the last three terms of (32) now correspond to the generating function of an harmonic oscillator of pulsation $\Omega_\varepsilon(q_1)$, in the variables $(\overline{q}_2, P_2)$. When V_0 does not depend on q_1 (decoupled case), we obtain a scheme on the fast variables which is always well defined, in contrast to (26). This property survives in the coupled situation. Indeed, inserting (32) in (5) yields an unconditionally well-defined symplectic scheme (see Algorithm 2.1). We denote it by $\Psi_h^{\mathrm{symp1}}(q_1,q_2,p_1,p_2)$. We note that this scheme is explicit, up to the inversion of the matrix $\Omega_\varepsilon(q_1)$ (which is a perturbation of the invertible matrix $\dfrac{\Omega}{\varepsilon}\mathrm{Id}_f$), and the inversion of the matrix in the left-hand side of (36). This latter matrix is always a perturbation of the identity, and thus invertible for h and ε sufficiently small.

Remark 2 *The generating function (32) is singular if* $\cos(h\Omega_\varepsilon(q_1)) = 0$. *This is reminiscent of the singularity of the generating function of an harmonic oscillator. Indeed, for* $H_{\mathrm{HO}}(q,p) = \dfrac{1}{2}(p^2+q^2)$, *the generating function writes*

$$S_{\mathrm{HO}}(t,q,P) = \left(\frac{P^2}{2} + \frac{q^2}{2}\right)\tan t + Pq\left(\frac{1}{\cos t} - 1\right).$$

It is singular when $\cos t = 0$. *Hence, it solves the Hamilton-Jacobi equation with initial condition at* $t = 0$ *formally only on* $t \in \left]-\dfrac{\pi}{2},\dfrac{\pi}{2}\right[$. *For any* q, p *and any* $t \notin \left(\dfrac{\pi}{2} + \pi\mathbb{Z}\right)$, *let us define* $Q(t;q,p)$ *and* $P(t;q,p)$ *by*

$$p = P(t;q,p) + \frac{\partial S_{\mathrm{HO}}}{\partial q}(t,q,P(t;q,p)), \quad Q(t;q,p) = q + \frac{\partial S_{\mathrm{HO}}}{\partial P}(t,q,P(t;q,p)). \tag{33}$$

One can check that the map $t \mapsto (Q(t;q,p), P(t;q,p))$ *can be extended to a* continuous *map* $\Psi(t)$ *defined on the* whole *set* $\mathbb{R}$*, and that* $\Psi(t)$ *solves the Newton equations obtained from* $H_{\rm HO}$ *with initial condition* (q,p) *on the* whole *set* $\mathbb{R}$*, and not only on* $\left]-\frac{\pi}{2},\frac{\pi}{2}\right[$*. Hence, even if* $S_{\rm HO}$ *is singular for some times* t*, we can still use it to define the flow* $(Q(t),P(t))$ *by (33) on the whole time line.*

In the case of (1), the fast variables dynamics is given by a perturbed fast harmonic oscillator. We observe that, even if (32) may be singular, the scheme obtained from (32) can be extended to a continuous *scheme. We will* observe *in Section 3.3 that this numerical flow is an accurate approximation of the exact flow, even if* $h \gg \varepsilon$*.*

Algorithm 2.1 (Symplectic Scheme $\Psi_h^{\rm symp1}(q_1,q_2,p_1,p_2)$)
Set $(q_1,q_2,p_1,p_2)=(q_1^n,q_2^n,p_1^n,p_2^n)$ and perform the following steps:

1. *Set* $\overline{q}_2 = q_2 + \dfrac{\varepsilon^2}{\Omega^2}\nabla_2 V_0(q_1,0)$.

2. *Set* $\Omega_\varepsilon(q_1) = \dfrac{\Omega}{\varepsilon}\,\mathrm{Id}_f + \dfrac{\varepsilon}{2\Omega}\nabla_{22}V_0(q_1,0)$ *and compute*

$$\begin{aligned} \widetilde{Q}_2 &= \cos(h\Omega_\varepsilon(q_1))\ \overline{q}_2 + \Omega_\varepsilon^{-1}(q_1)\sin(h\Omega_\varepsilon(q_1))\ p_2, &(34)\\ P_2 &= -\Omega_\varepsilon(q_1)\sin(h\Omega_\varepsilon(q_1))\ \overline{q}_2 + \cos(h\Omega_\varepsilon(q_1))\ p_2. &(35)\end{aligned}$$

3. *Solve for* $\overline{P}_1 \in \mathbb{R}^s$ *the equation*

$$\begin{aligned}\left(\mathrm{Id}_s + \frac{h^2}{2}\nabla_{11}V_0 - \frac{\varepsilon^2 h}{\Omega^2}P_2^T\nabla_{112}V_0\right)\overline{P}_1 = p_1 - \frac{\varepsilon^2}{\Omega^2}\nabla_{12}V_0 p_2 \\ -h\left(\nabla_1 V_0 - \frac{\varepsilon^2}{\Omega^2}\nabla_{12}V_0\nabla_2 V_0\right) + \frac{h^2\varepsilon^2}{2\Omega^2}P_2^T\nabla_{112}V_0\nabla_1 V_0 - \kappa, \quad (36)\end{aligned}$$

with κ defined by

$$\forall 1\le j\le s,\quad \kappa_j = \frac{\varepsilon}{2\Omega}\int_0^h x_2(t)^T\ \frac{\partial\nabla_{22}V_0}{\partial q_{1j}}\ \Omega_\varepsilon(q_1)\ x_2(t)\ dt, \qquad (37)$$

where $x_2(t) = \cos(t\Omega_\varepsilon(q_1))\ \overline{q}_2 + \Omega_\varepsilon^{-1}(q_1)\sin(t\Omega_\varepsilon(q_1))\ p_2$. In (36) and (37), all the derivatives of V_0 are evaluated at $(q_1,0)$.

4. *Set* $\quad P_1 = \overline{P}_1 + \dfrac{\varepsilon^2}{\Omega^2}\nabla_{12}V_0(q_1,0)P_2 \quad$ *and* $\quad Q_1 = q_1 + h\overline{P}_1 + \dfrac{h^2}{2}\nabla_1 V_0(q_1,0)$.

5. *Set* $\quad Q_2 = \widetilde{Q}_2 - \dfrac{\varepsilon^2}{\Omega^2}\nabla_2 V_0(q_1,0) - \dfrac{\varepsilon^2}{\Omega^2}\nabla_{12}V_0(q_1,0)\left(h\overline{P}_1 + \dfrac{h^2}{2}\nabla_1 V_0(q_1,0)\right)$.

Set $\left(q_1^{n+1},q_2^{n+1},p_1^{n+1},p_2^{n+1}\right) = (Q_1,Q_2,P_1,P_2)$.

Remark 3 *High-order derivatives of V_0 appear in Algorithm 2.1. This originates from the strategy of approximating the generating function in order to derive a numerical scheme. This was already observed by Feng [12] for nonstiff hamiltonian functions of the form $\dfrac{p^T p}{2} + V(q)$. Replacing such high-order derivatives by their finite difference approximation is a possible option, which however breaks the symplecticity of the scheme if it is done on the scheme itself. Another option is to make this finite difference approximation directly in the generating function, and from there derive a symplectic scheme following (5). We will not pursue in this direction in the present work.*

Remark 4 *When V_0 does not depend on q_2, the fast variables are decoupled from the slow ones. For the fast variables (q_2, p_2), the scheme Ψ_h^{symp1} is an exact integration.*

The scheme $\Psi_h^{\mathrm{symp1}}(q_1, q_2, p_1, p_2)$ requires the computation of the matrices $\sin(h\Omega_\varepsilon(q_1))$ and $\cos(h\Omega_\varepsilon(q_1))$. When the dimension f associated to the fast degrees of freedom is small, such a computation is easy. On the other hand, if the dimension f is high, then such a computation can be expensive. For the rest of Section 2.1, we assume that f is indeed large and show a possible manner to approximate these matrices, so that their exact computation is not necessary.

Suppose that we have two approximations s_ε^a and s_ε^b of $\sin(h\Omega_\varepsilon(q_1))$, and an approximation c_ε of $\cos(h\Omega_\varepsilon(q_1))$. Assume that s_ε^a, s_ε^b and c_ε are symmetric matrices, that s_ε^a, s_ε^b, c_ε and $\Omega_\varepsilon(q_1)$ commute, and that $c_\varepsilon^2 + s_\varepsilon^a s_\varepsilon^b = \mathrm{Id}_f$. Replacing (32) by the following *modified* approximation:

$$\boxed{\begin{array}{rcl} S_\varepsilon^{\mathrm{symp2}}(h) & = & h\left[V_0(q_1,0) - \dfrac{\varepsilon^2}{2\Omega^2}\left(\nabla_2 V_0(q_1,0)\right)^T \nabla_2 V_0(q_1,0) + \dfrac{1}{2}\overline{P}_1^T\overline{P}_1\right] \\ & + & \dfrac{h^2}{2}(\nabla_1 V_0(q_1,0))^T\overline{P}_1 \\ & + & \dfrac{1}{2}P_2^T\Omega_\varepsilon^{-1}(q_1)s_\varepsilon^a\, c_\varepsilon^{-1}\, P_2 + \dfrac{1}{2}\bar{q}_2^T\Omega_\varepsilon(q_1)s_\varepsilon^b\, c_\varepsilon^{-1}\,\overline{q}_2 + P_2^T(c_\varepsilon^{-1} - \mathrm{Id}_f)\,\overline{q}_2, \end{array}} \tag{38}$$

next inserting (38) in (5), we obtain

$$P_2 = c_\varepsilon p_2 - s_\varepsilon^b\,\Omega_\varepsilon(q_1)\overline{q}_2, \tag{39}$$

$$Q_2 = \widetilde{Q}_2 - \frac{\varepsilon^2}{\Omega^2}\nabla_2 V_0(q_1,0) - \frac{\varepsilon^2}{\Omega^2}\nabla_{12}V_0(q_1,0)\left(h\overline{P}_1 + \frac{h^2}{2}\nabla_1 V_0(q_1,0)\right), \tag{40}$$

with

$$\widetilde{Q}_2 = c_\varepsilon\overline{q}_2 + s_\varepsilon^a\,\Omega_\varepsilon^{-1}(q_1)p_2. \tag{41}$$

We recognize in formulae (39) and (41) an approximation of the solution, at time h, of the equation

$$\frac{dx_2}{dt} = y_2, \quad \frac{dy_2}{dt} = -\Omega_\varepsilon^2(q_1)x_2, \quad (x_2, y_2) \in \mathbb{R}^f \times \mathbb{R}^f, \quad (x_2^0, y_2^0) = (\overline{q}_2, p_2). \tag{42}$$

Note that we have used the exact solution of this system in Algorithm 2.1, see (34) and (35). This suggests the following numerical strategy:

- we first integrate the auxiliary problem (42) by the velocity Verlet scheme with the time step $h_\mu = h/k$ ($k \in \mathbb{N}^*$). At the time step k, the exact solution $(x_2(h = kh_\mu), y_2(h = kh_\mu))$ is thus approximated by (x_2^k, y_2^k), with

$$\begin{pmatrix} x_2^k \\ y_2^k \end{pmatrix} = \begin{pmatrix} u_k & v_k \\ -w_k & u_k \end{pmatrix} \begin{pmatrix} x_2^0 \\ y_2^0 \end{pmatrix}, \tag{43}$$

  where u_k, v_k and w_k are three matrices of size $f \times f$.

- We next set $s_\varepsilon^a = \Omega_\varepsilon(q_1)\, v_k$, $s_\varepsilon^b = \Omega_\varepsilon^{-1}(q_1)\, w_k$ and $c_\varepsilon = u_k$ (note that these three matrices satisfy the above assumptions), and we proceed with the calculation of P and Q using the $S_\varepsilon^{\mathrm{symp2}}$ obtained.

Following these lines, we obtain from the generating function $S_\varepsilon^{\mathrm{symp2}}$ a symplectic scheme, called Ψ_h^{symp2} in the sequel (see Algorithm 2.2).

Algorithm 2.2 (Symplectic Scheme $\Psi_h^{\mathrm{symp2}}(q_1, q_2, p_1, p_2)$)
Set $(q_1, q_2, p_1, p_2) = (q_1^n, q_2^n, p_1^n, p_2^n)$ and perform the following steps:

1. *Proceed with Step 1 of Algorithm 2.1.*
2. *Set* $\Omega_\varepsilon(q_1) = \dfrac{\Omega}{\varepsilon}\,\mathrm{Id}_f + \dfrac{\varepsilon}{2\Omega}\nabla_{22}V_0(q_1,0)$ *and numerically integrate*

$$\frac{dx_2}{dt} = y_2, \quad \frac{dy_2}{dt} = -\Omega_\varepsilon^2(q_1)x_2, \quad (x_2^0, y_2^0) = (\overline{q}_2, p_2), \tag{44}$$

   with the velocity Verlet scheme, with a time step $h_\mu = h/k$ ($k \in \mathbb{N}^*$) for k steps. Set $(\widetilde{Q}_2, P_2) = (x_2^k, p_2^k)$.
3. *Solve for $\overline{P}_1$ the equation (36), where now κ is defined by*

$$\kappa_j = \frac{\varepsilon}{2\Omega}\frac{h_\mu}{2}\sum_{n=0}^{k-1}\left((x_2^n)^T\ \frac{\partial\nabla_{22}V_0}{\partial q_{1j}}\ \Omega_\varepsilon(q_1)\ x_2^n + (x_2^{n+1})^T\ \frac{\partial\nabla_{22}V_0}{\partial q_{1j}}\ \Omega_\varepsilon(q_1)\ x_2^{n+1}\right) \tag{45}$$

   for all $1 \le j \le s$, where $(x_2^n)_{0\le n\le k}$ is the numerical solution of (44) and where all the derivatives of V_0 are evaluated at $(q_1, 0)$.
4. *Proceed with Step 4 of Algorithm 2.1.*
5. *Proceed with Step 5 of Algorithm 2.1.*

Set $\left(q_1^{n+1}, q_2^{n+1}, p_1^{n+1}, p_2^{n+1}\right) = (Q_1, Q_2, P_1, P_2)$.

It is interesting to note that making use of (38) instead of (32) (for instance because the dimension f is too large for $\sin(h\Omega_\varepsilon(q_1))$ and $\cos(h\Omega_\varepsilon(q_1))$ to be computed explicitly) amounts to numerically integrating system (42) (as opposed to exactly integrating it for (32), see (34) and (35)). Then the definition (37) of κ (in which the exact solution $x_2(t)$ of (42) enters) is to be replaced by (45), which requires the numerical solution of (42). In addition, we can see that (45) is an approximation by a trapezoidal rule of (37). The fact that (37) is approximated by a trapezoidal rule is consistent with the fact that (42) is integrated by the velocity Verlet algorithm.

Remark 5 *Our approach to compute P_2 and Q_2 is thus somewhat similar to the Impulse algorithm [16, 35], and to algorithms that have been proposed in the same spirit [10, 13, 27,*

29, 33, 34]: we numerically integrate a fast equation on the time interval $[0, h]$*, and we use this numerical solution in the slow scheme of step* $h \gg \varepsilon$*. Note however that the pulsation of the fast equation (42) is* $\Omega_\varepsilon(q_1)$*, whereas the pulsation of the original fast problem is* Ω/ε*. So the fast problem (42) that we consider here is different from the fast problem considered by the Impulse algorithm.*

2.2 Non-symplectic variants

The expressions for Q_2 and Q_1 in both schemes $\Psi_h^{\rm symp1}$ (see Algorithm 2.1) and $\Psi_h^{\rm symp2}$ (see Algorithm 2.2) read

$$\begin{aligned} Q_1 &= q_1 + h\overline{P}_1 + \frac{h^2}{2}\nabla_1 V_0(q_1, 0), \\ Q_2 &= \widetilde{Q}_2 - \frac{\varepsilon^2}{\Omega^2}\nabla_2 V_0(q_1, 0) - \frac{\varepsilon^2}{\Omega^2}\nabla_{12} V_0(q_1, 0)\left(h\overline{P}_1 + \frac{h^2}{2}\nabla_1 V_0(q_1, 0)\right), \end{aligned} \tag{46}$$

where the actual expression for $\widetilde{Q}_2$ depends on whether $\Psi_h^{\rm symp1}$ or $\Psi_h^{\rm symp2}$ is considered. On these formulae, we observe that

$$Q_2 = \widetilde{Q}_2 - \frac{\varepsilon^2}{\Omega^2}\nabla_2 V_0(Q_1, 0) + O(\varepsilon^2 h^2). \tag{47}$$

Note that, in (47), $\nabla_2 V_0$ is evaluated at Q_1 in contrast to (46) where it is evaluated at q_1. We interpret (47) as the change of variable dual to (31). We thus introduce two new schemes, $\Psi_h^{\rm Nsymp1}$ and $\Psi_h^{\rm Nsymp2}$ (see Algorithms 2.3 and 2.4), replacing (46) by

$$Q_2 = \widetilde{Q}_2 - \frac{\varepsilon^2}{\Omega^2}\nabla_2 V_0(Q_1, 0)$$

in respectively the schemes $\Psi_h^{\rm symp1}$ and $\Psi_h^{\rm symp2}$. Since these schemes are not obtained from a generating function, it is very likely that they are not symplectic. The main motivation for their introduction is their very good numerical performances, which will be reported on in Section 3.

Algorithm 2.3 (Non-symplectic Scheme $\Psi_h^{\rm Nsymp1}(q_1, q_2, p_1, p_2)$)
Set $(q_1, q_2, p_1, p_2) = (q_1^n, q_2^n, p_1^n, p_2^n)$ *and perform the following steps:*

1. *Proceed with Steps 1 to 4 of Algorithm 2.1.*
2. *Set* $Q_2 = \widetilde{Q}_2 - \dfrac{\varepsilon^2}{\Omega^2}\nabla_2 V_0(Q_1, 0).$

Set $\left(q_1^{n+1}, q_2^{n+1}, p_1^{n+1}, p_2^{n+1}\right) = (Q_1, Q_2, P_1, P_2).$

Algorithm 2.4 (Non-symplectic Scheme $\Psi_h^{\mathrm{Nsymp2}}(q_1,q_2,p_1,p_2)$)
Set $(q_1,q_2,p_1,p_2)=(q_1^n,q_2^n,p_1^n,p_2^n)$ *and perform the following steps:*

1. *Proceed with Steps 1 to 4 of Algorithm 2.2.*

2. *Set* $\quad Q_2=\widetilde{Q}_2-\dfrac{\varepsilon^2}{\Omega^2}\nabla_2 V_0(Q_1,0).$

Set $\left(q_1^{n+1},q_2^{n+1},p_1^{n+1},p_2^{n+1}\right)=(Q_1,Q_2,P_1,P_2).$

2.3 Preconditioning by the fast motion: new symplectic schemes

In Sections 2.1 and 2.2, we have manipulated the original variables (q_1,q_2,p_1,p_2) of the dynamics. We now describe a similar approach developed *after* a preliminary change of variables. The latter approach is again suggested by the consideration of the uncoupled case. Indeed, assume momentarily that V_0 does not depend on q_2. Then the fast and the slow variables are decoupled, and we can analytically integrate the fast motion. Such an observation is also used in the exponential integrators analyzed in [21, Chap. XIII], in the integrator described in [15], and in the adiabatic integrators [25, 26] addressing the case of a frequency matrix that varies with q_1. The first step of these algorithms is indeed a change of variables, so that the new variables are solutions of an EDO simpler than the original one.

Consider the time-dependent change of variables $(q_2,p_2)\mapsto(x_2,y_2)=\chi(t,q_2,p_2)$ defined by

$$\begin{aligned} q_2 &= \cos\left(\frac{\Omega t}{\varepsilon}\right)x_2+\frac{\varepsilon}{\Omega}\sin\left(\frac{\Omega t}{\varepsilon}\right)y_2,\\ p_2 &= -\frac{\Omega}{\varepsilon}\sin\left(\frac{\Omega t}{\varepsilon}\right)x_2+\cos\left(\frac{\Omega t}{\varepsilon}\right)y_2. \end{aligned}$$

Then $(x_2(t),y_2(t))=\chi(t,q_2(t),p_2(t))$ are constant functions when $\partial_2 V_0\equiv 0$. More generally, the dynamics on (x_2,y_2) reads

$$\begin{aligned} \dot{x}_2 &= \frac{\varepsilon}{\Omega}\sin\left(\frac{\Omega t}{\varepsilon}\right)\partial_2 V_0\left[q_1,\cos\left(\frac{\Omega t}{\varepsilon}\right)x_2(t)+\frac{\varepsilon}{\Omega}\sin\left(\frac{\Omega t}{\varepsilon}\right)y_2(t)\right],\\ \dot{y}_2 &= -\cos\left(\frac{\Omega t}{\varepsilon}\right)\partial_2 V_0\left[q_1,\cos\left(\frac{\Omega t}{\varepsilon}\right)x_2(t)+\frac{\varepsilon}{\Omega}\sin\left(\frac{\Omega t}{\varepsilon}\right)y_2(t)\right]. \end{aligned}$$

The dynamics on (q_1,x_2,p_1,y_2) is a hamiltonian dynamics with the time-dependent hamiltonian

$$H_\varepsilon^{\mathrm{pre}}(t,q_1,x_2,p_1,y_2)=\frac{p_1^T p_1}{2}+W_\varepsilon\left(\frac{\Omega t}{\varepsilon},q_1,x_2,y_2\right),$$

with

$$W_\varepsilon(\tau,q_1,x_2,y_2)=V_0\left[q_1,(\cos\tau)x_2+\frac{\varepsilon}{\Omega}(\sin\tau)y_2\right].$$

Let us now take this Hamiltonian, as a function of (q_1, x_2, p_1, y_2), as a starting point for our manipulations of Section 2.1. Let $\overline{S}_\varepsilon(t, q_1, x_2, P_1, Y_2)$ solve

$$\partial_t \overline{S}_\varepsilon = \frac{P_1^T P_1}{2} + W_\varepsilon \left(\frac{\Omega t}{\varepsilon}, q_1 + \partial_{P_1} \overline{S}_\varepsilon, x_2 + \partial_{P_2} \overline{S}_\varepsilon, Y_2 \right), \quad \overline{S}_\varepsilon(0, q_1, x_2, P_1, Y_2) = 0.$$

The variable x_2 is of order ε, so we again change the variables and the unknown function:

$$r_2 = \frac{\Omega}{\varepsilon} x_2 \quad \text{and} \quad S_\varepsilon(t, q_1, r_2, P_1, Y_2) = \overline{S}_\varepsilon \left(t, q_1, \frac{\varepsilon r_2}{\Omega}, P_1, Y_2 \right),$$

so that S_ε satisfies

$$\partial_t S_\varepsilon = \frac{P_1^T P_1}{2} + W_\varepsilon \left(\frac{\Omega t}{\varepsilon}, q_1 + \partial_{P_1} S_\varepsilon, \frac{\varepsilon r_2}{\Omega} + \partial_{P_2} S_\varepsilon, Y_2 \right), \quad S_\varepsilon(0, q_1, r_2, P_1, Y_2) = 0. \tag{48}$$

We make the Ansatz

$$\begin{aligned} S_\varepsilon(t, q_1, r_2, P_1, Y_2) &= S_0(t, \tau, q_1, r_2, P_1, Y_2) + \varepsilon S_1(t, \tau, q_1, r_2, P_1, Y_2) \\ &+ \text{higher order terms in } \varepsilon^k,\ k \geq 2, \end{aligned} \tag{49}$$

where the fast time τ is again $\tau = \dfrac{t\Omega}{\varepsilon}$, and where the functions $(S_k)_{k\geq 0}$ are supposed to be 2π periodic in τ. We now insert (49) in (48), identify the first variable of W_ε with the fast time τ, and expand in powers of ε.

The fast position is of order ε, so S_0 does not depend on Y_2. From the equation of order ε^{-1}, we infer that S_0 does not depend on τ. The equation of order ε^0 reads

$$\partial_t S_0 + \Omega \partial_\tau S_1 = \frac{P_1^T P_1}{2} + V_0(q_1 + \partial_{P_1} S_0, 0). \tag{50}$$

Since S_0 does not depend on τ and S_1 is 2π periodic in τ, we infer from (50) that

$$\partial_t S_0 = \frac{P_1^T P_1}{2} + V_0(q_1 + \partial_{P_1} S_0, 0) \tag{51}$$

and

$$\partial_\tau S_1 = 0. \tag{52}$$

Equation (51) is supplied with the initial condition $S_0(t = 0, q_1, r_2, P_1) = 0$. For each r_2, we thus recognize the Hamilton-Jacobi equation for the hamiltonian function

$$H_1 = \frac{p_1^T p_1}{2} + V_0(q_1, 0). \tag{53}$$

So S_0 does not depend on r_2. In the sequel, we will approximate $S_0(t, q_1, P_1)$ by

$$S_0(t, q_1, P_1) \approx S_0^{\mathrm{SE}}(t, q_1, P_1),$$

with

$$S_0^{\rm SE}(t,q_1,P_1) = S_0(0,q_1,P_1) + t\partial_t S_0(0,q_1,P_1) = t\left(\frac{P_1^T P_1}{2} + V_0(q_1,0)\right), \qquad (54)$$

which amounts to integrating the hamiltonian dynamics generated by (53) with the symplectic Euler algorithm. We have: $S_0(t) = S_0^{\rm SE}(t) + O(t^2)$.

The sequel of the identification is carried out in details in Appendix 6 (see in particular (95) and (102)). We find that

$$S_1 \equiv 0 \qquad (55)$$

and that $S_2(t) = S_2^{\rm SE}(t) + O(t^2)$, with

$$\begin{aligned} S_2^{\rm SE}(t,\tau,q_1,r_2,P_1,Y_2) &= \frac{1}{\Omega^2}(\nabla_2 V_0)^T Y_2 - \frac{t}{2\Omega^2}(\nabla_2 V_0)^T \nabla_2 V_0 \\ &+ \frac{t}{4\Omega^2}\left(r_2^T \nabla_{22} V_0 r_2 + Y_2^T \nabla_{22} V_0 Y_2\right) \\ &+ \frac{1}{\Omega^2}(\nabla_2 V_0(q_1+tP_1,0))^T\left((\sin\tau) r_2 - (\cos\tau) Y_2\right), \end{aligned} \qquad (56)$$

where the derivatives of V_0 are evaluated at $(q_1,0)$ unless otherwise mentioned.

From then on, the procedure is similar to that followed in Section 2.1, up to some details that we now highlight. Consider the approximation

$$S_\varepsilon(h) = S_0(h) + \varepsilon S_1(h) + \varepsilon^2 S_2(h) + \ldots \approx S_\varepsilon^{\rm pre1}(h)$$

with

$$\boxed{S_\varepsilon^{\rm pre1}(h) := S_0^{\rm SE}(h) + \varepsilon S_1(h) + \varepsilon^2 S_2^{\rm SE}(h),} \qquad (57)$$

where $S_0^{\rm SE}$, S_1 and $S_2^{\rm SE}$ are respectively defined by (54), (55) and (56). We insert this approximation in (5) and obtain the following *implicit* equations for (P_1,Y_2) (as opposed to the *explicit* equations that we obtained in Section 2.1):

$$\begin{aligned} y_2 &= Y_2 + \frac{h\varepsilon}{2\Omega}\nabla_{22} V_0(q_1,0) r_2 + \frac{\varepsilon}{\Omega}\sin\tau \nabla_2 V_0(q_1+hP_1,0), \\ p_1 &= P_1 + h\nabla_1 V_0(q_1,0) + \frac{\varepsilon^2}{\Omega^2}\nabla_{12} V_0(q_1,0) Y_2 - \frac{h\varepsilon^2}{\Omega^2}\nabla_{12} V_0(q_1,0)\nabla_2 V_0(q_1,0) \\ &+ \frac{h\varepsilon^2}{4\Omega^2}(r_2^T \nabla_{122} V_0(q_1,0) r_2 + Y_2^T \nabla_{122} V_0(q_1,0) Y_2) \\ &+ \frac{\varepsilon^2}{\Omega^2}\nabla_{12} V_0(q_1+hP_1,0)\left((\sin\tau) r_2 - (\cos\tau) Y_2\right). \end{aligned}$$

This implicit system reads $z = Z + hf(z,Z) + \varepsilon g(z,Z)$ with $z = (p_1,y_2)$, and thus a fixed point method works well to compute $Z = (P_1,Y_2)$. Next, we compute (Q_1,X_2) by explicit formulae. Returning to the original variables (q_1,q_2,p_1,p_2), we write the obtained scheme, which is symplectic, as $(Q_1,Q_2,P_1,P_2) = \Psi_h^{\rm pre1}(q_1,q_2,p_1,p_2)$ (see Algorithm 2.5).

Algorithm 2.5 (Preconditioned Symplectic Scheme $\Psi_h^{\mathrm{pre1}}(q_1,q_2,p_1,p_2)$)
Set $(q_1,q_2,p_1,p_2)=(q_1^n,q_2^n,p_1^n,p_2^n)$, $\tau=\Omega h/\varepsilon$ and perform the following steps:

1. *Change of variables: set* $x_2=q_2,\quad y_2=p_2,\quad r_2=\Omega x_2/\varepsilon.$

2. *Solve for (P_1,Y_2) the equations*

$$\left\{\begin{array}{rcl} y_2 &=& Y_2+\dfrac{h\varepsilon}{2\Omega}\nabla_{22}V_0(q_1,0)r_2+\dfrac{\varepsilon}{\Omega}\sin\tau\nabla_2V_0(q_1+hP_1,0),\\ p_1 &=& P_1+h\nabla_1V_0(q_1,0)+\dfrac{\varepsilon^2}{\Omega^2}\nabla_{12}V_0(q_1,0)Y_2\\ &-& \dfrac{h\varepsilon^2}{\Omega^2}\nabla_{12}V_0(q_1,0)\nabla_2V_0(q_1,0)\\ &+& \dfrac{h\varepsilon^2}{4\Omega^2}(r_2^T\nabla_{122}V_0(q_1,0)r_2+Y_2^T\nabla_{122}V_0(q_1,0)Y_2)\\ &+& \dfrac{\varepsilon^2}{\Omega^2}\nabla_{12}V_0(q_1+hP_1,0)\left((\sin\tau)r_2-(\cos\tau)Y_2\right). \end{array}\right.$$

3. *Set* $Q_1=q_1+hP_1+\dfrac{h\varepsilon^2}{\Omega^2}\nabla_{12}V_0(q_1+hP_1,0)\left((\sin\tau)r_2-(\cos\tau)Y_2\right).$

4. *Set*

$$X_2=x_2+\frac{\varepsilon^2}{\Omega^2}\nabla_2V_0(q_1,0)+\frac{h\varepsilon^2}{2\Omega^2}\nabla_{22}V_0(q_1,0)Y_2-\frac{\varepsilon^2}{\Omega^2}\cos\tau\nabla_2V_0(q_1+hP_1,0).$$

5. *Return to the original variables:*

$$\left\{\begin{array}{rcl} Q_2 &=& (\cos\tau)X_2+\dfrac{\varepsilon}{\Omega}(\sin\tau)Y_2,\\ P_2 &=& -\dfrac{\Omega}{\varepsilon}(\sin\tau)X_2+(\cos\tau)Y_2. \end{array}\right.$$

Set $\left(q_1^{n+1},q_2^{n+1},p_1^{n+1},p_2^{n+1}\right)=(Q_1,Q_2,P_1,P_2).$

Neglecting all terms of order ε^3, the scheme $\Psi_h^{\mathrm{pre1}}(q_1,q_2,p_1,p_2)$ is of order 1 in h. A simple, well-known, manner to get a scheme of higher order is to consider the symmetric form

$$(Q_1,Q_2,P_1,P_2)=\Psi_h^{\mathrm{pre2}}(q_1,q_2,p_1,p_2)=\left(\Psi_{h/2}^{\mathrm{pre1}}\right)^*\ \Psi_{h/2}^{\mathrm{pre1}}(q_1,q_2,p_1,p_2).$$

This scheme is symplectic and, neglecting all terms of order ε^3, it is of order 2 in h (see Algorithm 2.6). Note that, if V_0 does not depend on q_2, then the slow and the fast variables are decoupled, and we recover the velocity Verlet algorithm in the slow variables and the exact flow in the fast variables.

Algorithm 2.6 (Preconditioned Symplectic Scheme $\Psi_h^{\rm pre2}(q_1,q_2,p_1,p_2)$)
Set $(q_1,q_2,p_1,p_2)=(q_1^n,q_2^n,p_1^n,p_2^n)$ *and perform the following steps:*

1. *Set* $(\overline{Q}_1,\overline{Q}_2,\overline{P}_1,\overline{P}_2)=\Psi_{h/2}^{\rm pre1}(q_1,q_2,p_1,p_2)$.

2. *Set* $(Q_1,Q_2,P_1,P_2)=\left(\Psi_{h/2}^{\rm pre1}\right)^*(\overline{Q}_1,\overline{Q}_2,\overline{P}_1,\overline{P}_2)$.

Set $\left(q_1^{n+1},q_2^{n+1},p_1^{n+1},p_2^{n+1}\right)=(Q_1,Q_2,P_1,P_2)$.

The major superiority of the scheme $\Psi_h^{\rm pre2}(q_1,q_2,p_1,p_2)$ on the scheme $\Psi_h^{\rm symp1}(q_1,q_2,p_1,p_2)$ is that there is no need to diagonalize the full matrix $\Omega_\varepsilon(q_1)$. In addition, the generating function $S_\varepsilon^{\rm pre1}(h)$ is never singular, in contrast to $S_\varepsilon^{\rm symp1}(h)$ (see Remark 2).

Let us conclude this section by the following remark, which concerns all the algorithms introduced. It is standard to show [3, 4] that the dynamics on the slow variables obtained in the limit $\varepsilon\to 0$ is a dynamics of hamiltonian $H_1=\dfrac{p_1^Tp_1}{2}+V_0(q_1,0)$. We show here that, in the limit $\varepsilon\to 0$, the algorithms introduced are consistent with this theoretical result. Let $S_{\rm slow}(t,q_1,P_1)$ be the solution of the Hamilton-Jacobi equation (10) associated to H_1. We observe that, in the limit $\varepsilon\to 0$, Algorithms 2.1 and 2.3 reduce for the slow variables to the symplectic algorithm that is derived from the generating function

$$S_{\rm slow}(0,q_1,P_1)+h\partial_t S_{\rm slow}(0,q_1,P_1)+\frac{h^2}{2}\partial_{tt}S_{\rm slow}(0,q_1,P_1),$$

which is indeed a converging approximation of $S_{\rm slow}(h,q_1,P_1)$. In the limit $\varepsilon\to 0$, Algorithm 2.5 reduces to the Symplectic Euler algorithm on H_1 (and Algorithm 2.6 reduces to the velocity Verlet algorithm). So, in the limit $\varepsilon\to 0$, all the algorithms introduced reduce to a symplectic scheme which integrates the limit dynamics.

Additionally, the time step h being fixed, we check that

$$\lim_{\varepsilon\to 0}\frac{P_2^TP_2+\Omega^2\ Q_2^TQ_2/(\varepsilon^2)}{p_2^Tp_2+\Omega^2\ q_2^Tq_2/(\varepsilon^2)}=1$$

for Algorithms 2.1, 2.3, 2.5 and 2.6, which is consistent with the fact that $\dfrac{p_2^Tp_2}{2}+\Omega^2\ \dfrac{q_2^Tq_2}{2\varepsilon^2}$ is an adiabatic invariant of the dynamics (see [3, 4]).

3 Numerical results

This section presents some numerical tests on the algorithms introduced in the previous section for the integration of (1)-(2) in the case of a constant fast frequency. We consider here Algorithms 2.1 and 2.3 (and their variants, Algorithms 2.2 and 2.4, when the fast

problem is numerically integrated), and Algorithm 2.6. All algorithms except Algorithms 2.3 and 2.4 are symplectic. We have also mentioned in the Introduction that symmetry may be an interesting property and wish to recall that only Algorithm 2.6 is symmetric.

The test-bed chosen for our comparison is the commonly used Fermi-Pasta-Ulam spring chain [21, Sec. XIII.2.1]. This chain is a collection of six one-dimensional springs: the even numbered springs are stiff and harmonic, whereas the odd numbered springs are nonharmonic and nonstiff. In this case, $q_1 = (q_{1,1}, q_{1,2}, q_{1,3}) \in \mathbb{R}^3$, $q_2 \in \mathbb{R}^3$, $\Omega(q_1) = 1$, and the potential energy V_0 in (1) reads

$$V_0 = \frac{1}{4}\left((q_{1,1} - q_{2,1})^4 + \sum_{i=1}^{2} (q_{1,i+1} - q_{2,i+1} - q_{1,i} - q_{2,i})^4 + (q_{1,3} + q_{2,3})^4 \right).$$

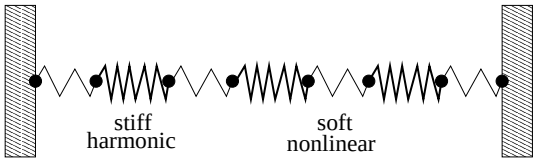

Figure 1: Fermi-Pasta-Ulam spring chain.

The energy is the fast spring j $(1 \leq j \leq 3)$ reads $I_j(q,p) = \dfrac{p_{2,j}^2}{2} + \dfrac{q_{2,j}^2}{2\varepsilon^2}$ and

$$I(q,p) = I_1(q,p) + I_2(q,p) + I_3(q,p) \tag{58}$$

is an adiabatic invariant in the sense of [21, Chap. XIII, Theorem 6.3].

In the following sections, we first study the performances of our algorithms as regards the computation of the exact trajectory. Following the practice of [21, Sec. XIII.2], we then compare our algorithms to the exponential integrators proposed in the literature. We name these various algorithms as in [21, Sec. XIII.2] and [15] (see Table 1).

Algorithm	Reference	Quality
A	Gautschi [14]	Non symplectic
B	Deuflhard [9] and Impulse algorithm [16, 35]	Symplectic
C	Garcia-Archilla *et al*, Mollify algorithm [13]	Symplectic
D	Hochbruck and Lubich [22]	Non symplectic
E	Hairer and Lubich [20]	Non symplectic
G	Grimm and Hochbruck [15]	Non symplectic

Table 1: Some exponential integrators proposed in the literature. All these integrators are symmetric.

3.1 Long time energy preservation

As mentioned in the Introduction, we cannot invoque backward error analysis to justify long time energy preservation for the symplectic algorithms proposed above. Indeed, these algorithms are useful in the regime where the time step is large compared to the shortest period present in the system. In the present state of our understanding, all we can do is therefore *test* them, that is numerically check that energy is well-preserved. This *a fortiori* applies to the non-symplectic variants we developed.

We work with $\varepsilon = 0.02$ and $h = 0.17$, and monitor the energy up to time $T = 10^6$, which is a rather large value compared to final times usually considered with this stiffness. The results obtained with Algorithms 2.1, 2.3 and 2.6 are shown on Figure 2. No energy drift can be seen.

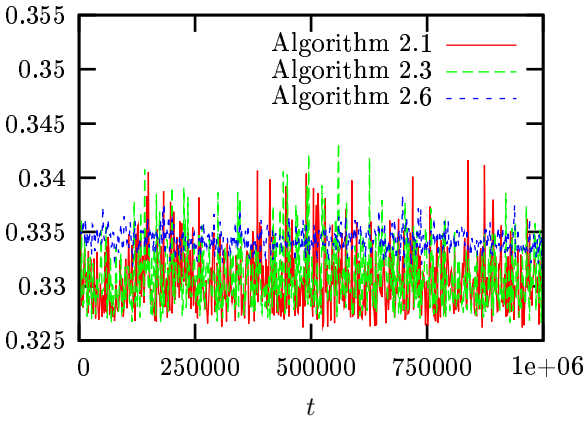

Figure 2: Energy per particle along the trajectory ($\varepsilon = 0.02$ and $h = 0.17$).

3.2 Exchange of fast energies

The sum $I(q,p)$ of the energies in the fast springs, given by (58), is an adiabatic invariant of the exact trajectory. Exchanges of energy between the fast springs occur on a time scale of order ε^{-1} (see [21, Sec. XIII.2.1]). We study how Algorithms 2.1, 2.3 and 2.6 reproduce this exchange.

Following [21, Fig. XIII.2.4], we set $\varepsilon = 0.02$ and $h = 0.03$. Results are shown on Figure 3. The exact trajectory and the numerically computed trajectories satisfactorily agree. We do not include the results for $\varepsilon = 10^{-3}$. They are similar, although the exchange (for both the exact and the approximated trajectories) is much slower.

Remark 6 *In the approximation (26), the term $\partial_t S_2$ is of paramount importance for the reproduction of the exchange of fast energies. If we remove this term from (26), we have*

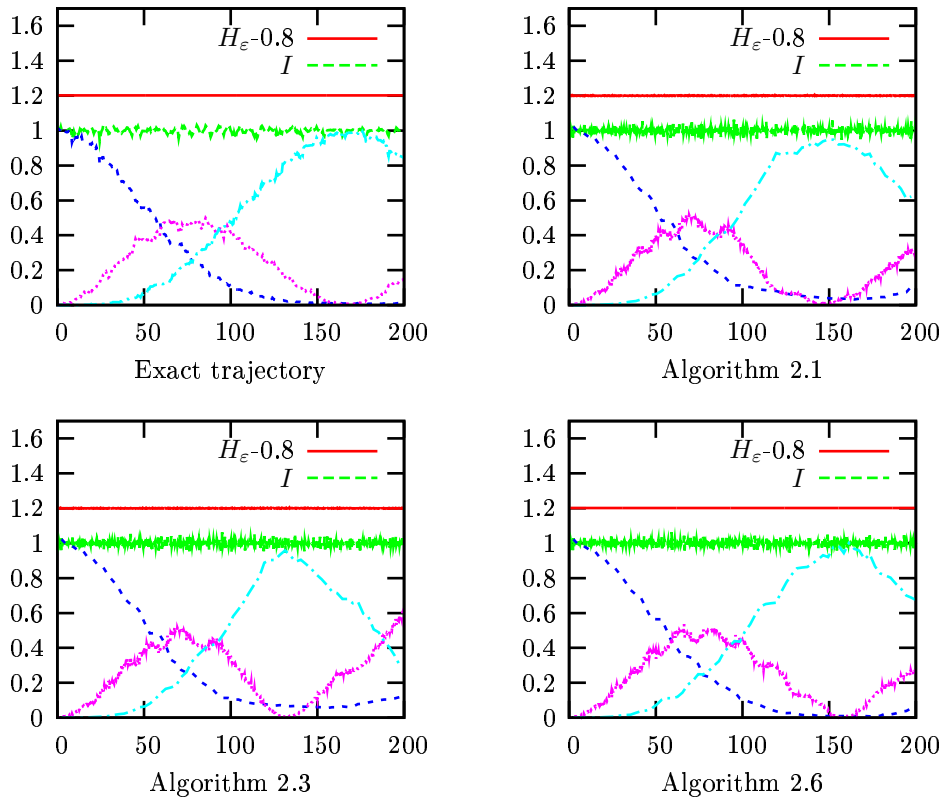

Figure 3: Preservation of the energy (for convenience, we plot $H_\varepsilon - 0.8$), of the adiabatic invariant I and exchange between the $\{I_j\}_{1\leq j\leq 3}$ for $\varepsilon = 0.02$ (all trajectories are computed with $h = 0.03$).

another generating function, from which we can derive an algorithm. We have checked that this latter algorithm poorly reproduces the exchanges of energy.

3.3 Comparison on a test case with a fixed stiffness

We now set $\varepsilon = 10^{-3}$, and study the performances of our algorithms when the time step h varies. We compare Algorithms 2.1, 2.3 and 2.6 with the exponential integrators described in [21, Chap. XIII] and in [15] (we omit in our comparison the Impulse algorithm (B), since it is usually outperformed by the Mollify algorithm (C); we have checked this in the particular situation considered here).

We first study the preservation of the energy and of the adiabatic invariant. On Figure 4, we plot, as a function of the time step h, the relative error

$$\text{err} = \max_{t\in[0,10^4]} \frac{|H_\varepsilon(t) - H_\varepsilon(0)|}{H_\varepsilon(0)} \tag{59}$$

on the energy conservation over the time interval $[0, 10^4]$. Note that the time frame $T = 10^4$ satisfies $T \gg \varepsilon^{-1}$. The motivation for such a choice will be explained in Remark 7.

On Figure 5, we plot

$$\max_{t\in[0,10^4]} \frac{|I_\varepsilon(t) - I_\varepsilon(0)|}{I_\varepsilon(0)}, \tag{60}$$

which is the maximum variation to the initial value of the adiabatic invariant. On the exact trajectory with $\varepsilon = 10^{-3}$, we observe that this quantity is close to 0.0037.

As is well-known [21, Fig. XIII.2.5], for several exponential integrators, resonances appear when h is a (odd or even or both) multiple of $\varepsilon\pi$, which is half the period of the fast motion. We also observe resonances with Algorithm 2.1. There are almost no resonances with Algorithms 2.3 and 2.6. However, for all the algorithms considered here, these resonances are very peaked: it is easy to find a time step h for which the algorithms are not resonant. We note that Algorithm 2.6 preserves the energy with an equal or better accuracy than all the other algorithms. Algorithms G, 2.3 and 2.6 have no resonances, and the latter two preserve the energy with a better accuracy than Algorithm G. We also observe that the adiabatic invariant variation (60) is very well reproduced by Algorithms 2.1, 2.3 and 2.6.

Remark 7 *We work with ε small. Indeed, when we compute an approximation of the generating function, we have made a truncation in the series in powers of ε (see (26), (32) and (38)). If ε is too large, this truncation does not make sense. Since ε is small, q_2 is also small, which implies that $V_0(q_1, q_2)$ could be well-approximated by a harmonic function of q_2, a test case that seems less challenging than the one with a V_0 function truly nonharmonic in q_2. However, despite its apparent simplicity, we observe that the test case at hand here is not so easy to deal with, since resonances appear with some of the algorithms. As already mentioned in the Introduction, we simulate the system over extremely long time frames (in practice, over $[0, T]$ with $T \gg \varepsilon^{-1}$), so that possible numerical instabilities could develop, if they had to.*

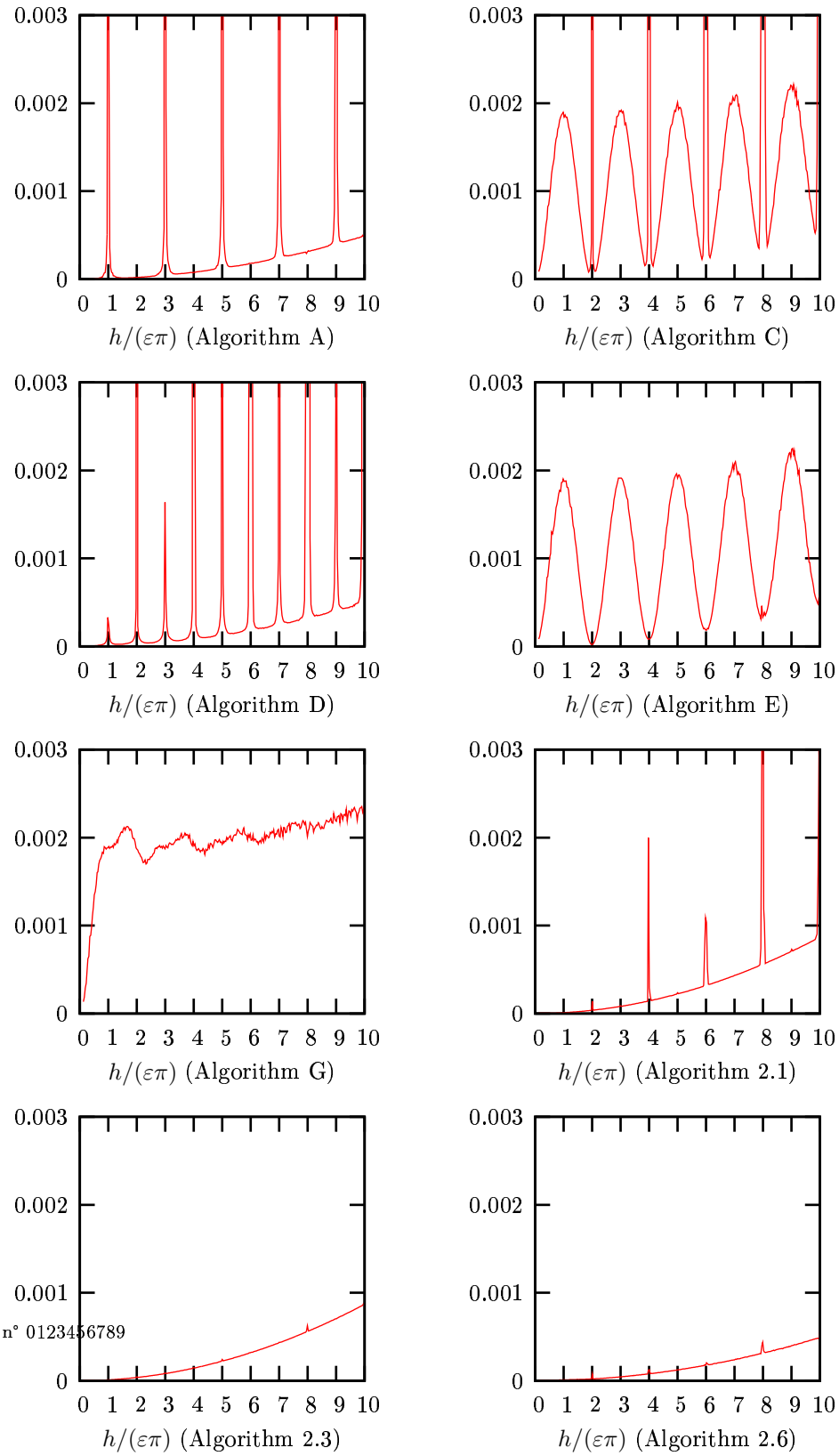

Figure 4: Maximum relative variation (59) of the energy on the time interval $[0, 10^4]$, for several time steps h ($\varepsilon = 10^{-3}$). See Table 1 for exponential algorithms terminology.

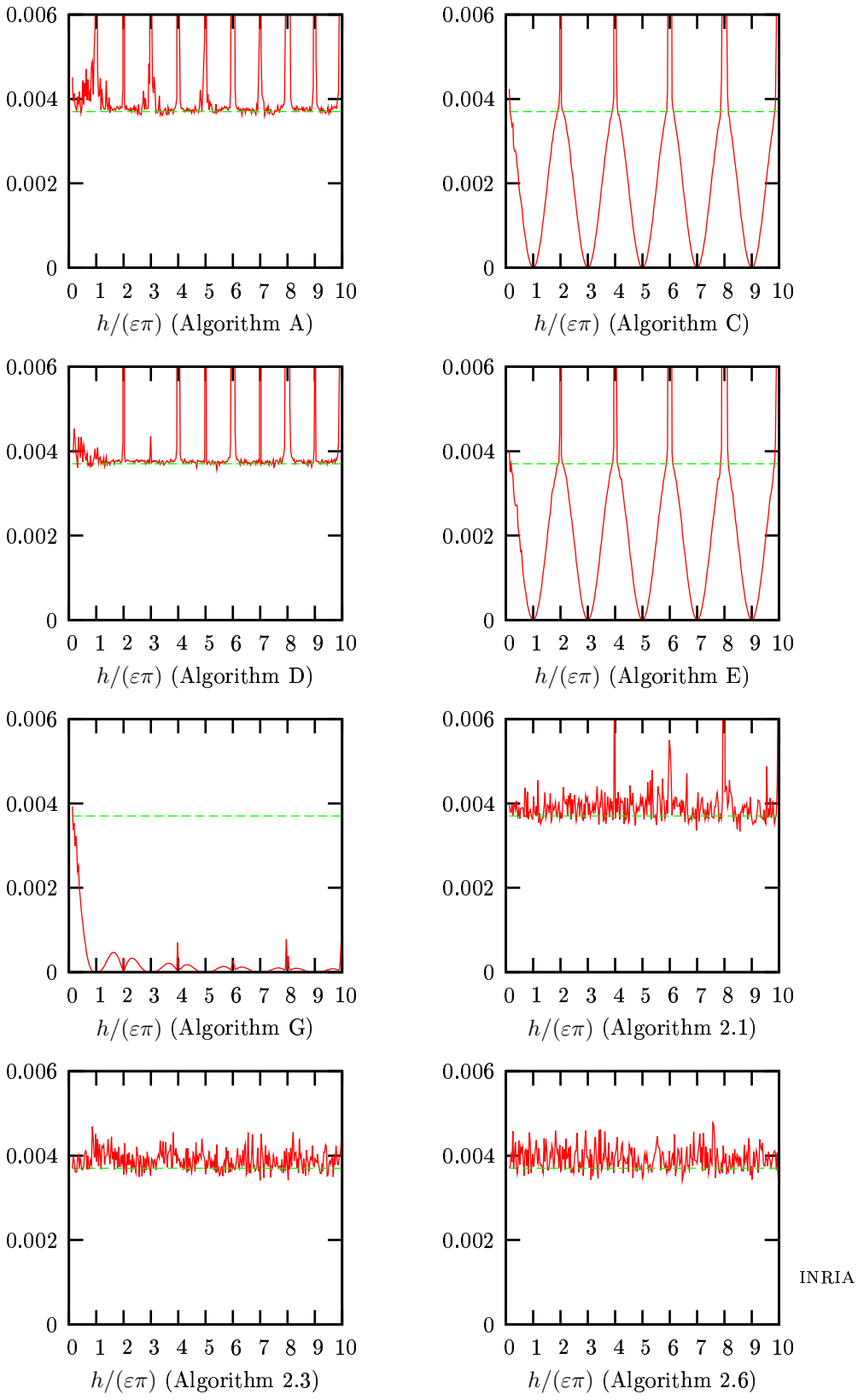

Figure 5: Maximum variation (60) of the adiabatic invariant on the time interval $[0, 10^4]$, for several time steps h ($\varepsilon = 10^{-3}$). We compare the numerical results with the exact result, which is here 0.0037 (see the body of the text). See Table 1 for exponential algorithms terminology.

We next study the global errors at time T, which we define by

$$\text{err} = \|x_{\text{num}}(T) - x_{\text{exact}}(T)\|_2 \tag{61}$$

for a variable $x \in \mathbb{R}^3$, where $\|\cdot\|_2$ is the Euclidean norm in $\mathbb{R}^3$, $x_{\text{exact}}(T)$ is the value of the variable x on the exact trajectory at time T and $x_{\text{num}}(T)$ is its approximation on the numerically computed trajectory. Following [15, Fig. 2], we study these errors at time $T = 1$, for the variable $x \equiv q_1$, $x \equiv q_2/\varepsilon$ (which is of order $O(1)$ in ε), $x \equiv p_1$ and $x \equiv p_2$. Results are shown on Figure 6. For the slow variables q_1 and p_1, we have gathered exponential algorithms for which the error was almost the same. For the fast variables q_2/ε and p_2, we have kept the two exponential algorithms that provide the smallest errors (see [15, Fig. 2] and [21, Fig. XIII.2.2] for more comprehensive numerical results).

We first see that, with Algorithms 2.1, 2.3 and 2.6, the error does not converge to 0 when $h \to 0$. This is due to the truncation in the series in powers of ε performed to approximate the generating function. Even if $h \to 0$, an error remains. Note however that we are not interested in the regime $h \to 0$, for numerical efficiency reasons.

As soon as $h \geq \varepsilon\pi$, we observe that the error on the slow variables q_1 and p_1 is similar for Algorithm 2.6 and for the exponential integrators A, C, D, E and G, provided we use a non-resonant time step for the latter algorithms. The error on q_1 and p_1 for Algorithms 2.1 and 2.3 is larger, but note that there is no resonance. We now turn to the fast variables. In the regime $h \geq \varepsilon\pi$ of practical interest, the error with Algorithms 2.1, 2.3 and 2.6 is much smaller that the error with the exponential integrators. There is no resonance with Algorithms 2.3 and 2.6. Apart from resonances, the accuracy of Algorithm 2.1 is similar to the accuracy of Algorithm 2.3. In summary, we observe a good accuracy on the solution at time $T = 1 \gg \varepsilon$ computed with the algorithms proposed here. Note that the time T is much longer than the time scale ε of the fast variables. Such a good accuracy on the slow variables is expected, but this is rather a surprise for the fast variables.

It is interesting to note that the accuracy observed in energy preservation with Algorithm 2.6 (better than that of exponential integrators) comes from a better accuracy on the fast variables. Algorithms 2.1 and 2.3 are also more accurate on the fast variables, but less on the slow variables. In addition, we observe that the resonances of Algorithm 2.1 come from the fast variables.

Let us emphasize that the conclusions drawn from the comparison between the algorithms developed in the present work and the algorithms A, C, D and E originate, and are limited to, the specific context considered. The algorithms A, C, D and E can be employed for *any* hamiltonian system with a slow/fast potential energy separation, whereas the algorithms introduced here apply to hamiltonians of the form (1). On the other hand, and this is then a fair comparison, Algorithms 2.1 to 2.6 outperform the G integrator, specifically developped for (1).

3.4 Robustness of the algorithms

Let us now compare the algorithms using a fixed time step $h = 0.02$, and a varying stiffness. Our aim is to check that the errors in the energy and adiabatic invariant preservations do

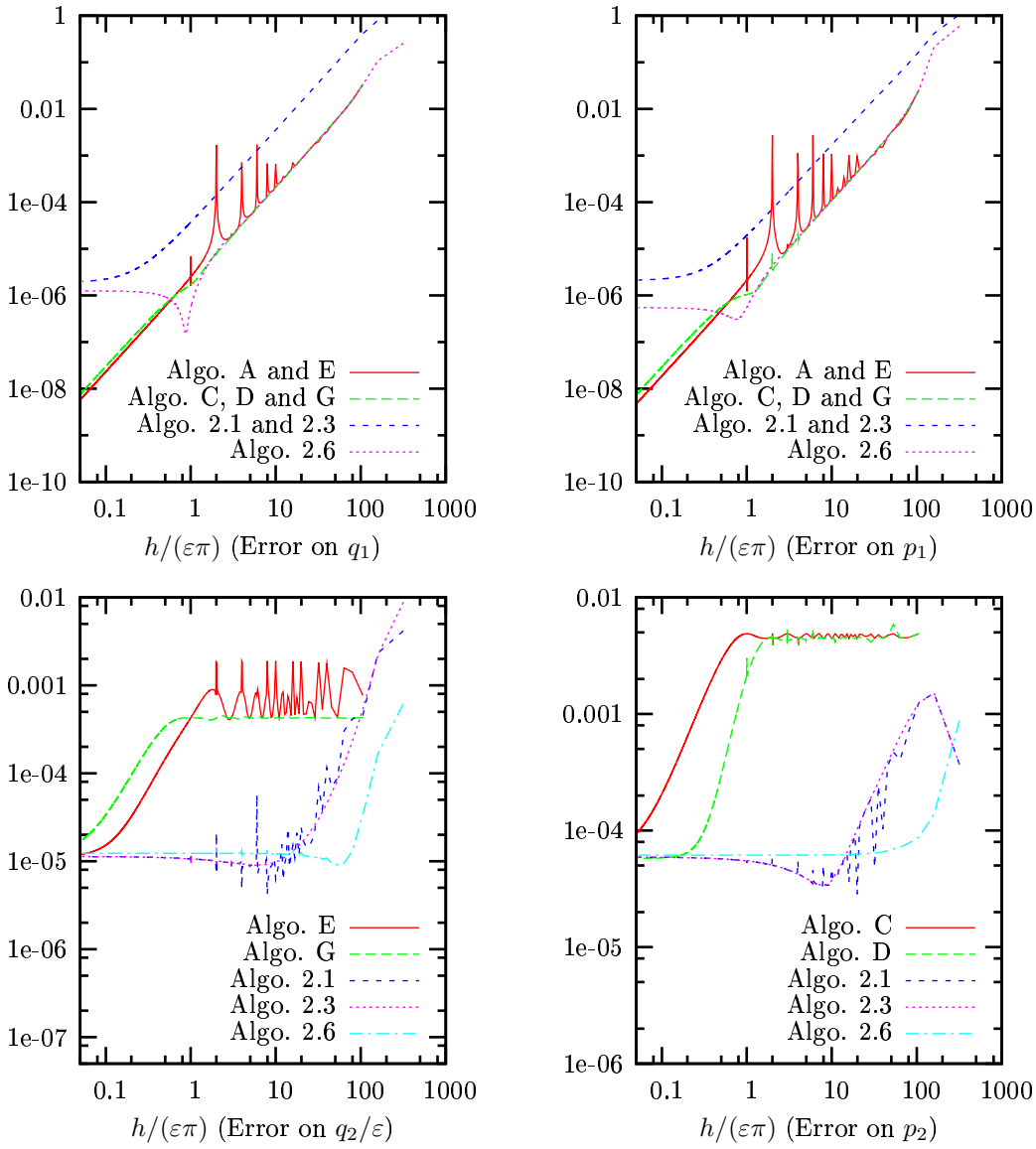

Figure 6: Global errors (61) at time $T = 1$, for several time steps h ($\varepsilon = 10^{-3}$). For the fast variables, only the results for the exponential integrators that best perform are shown. See Table 1 for exponential algorithms terminology.

not depend on ε, and thus that we can use a time step h which is not bounded by ε, as would be the case for the velocity-Verlet algorithm.

We use again the estimators (59) and (60). Results are shown on Figures 7 and 8. We again see that ε has to be sufficiently small for the energy to be well-preserved by Algorithms 2.1, 2.3 and 2.6. When ε is sufficiently small, we observe that the accuracy in the energy preservation does not depend on ε, so the algorithms are unsensitive to the stiffness, up to the occurence of resonances. The variations of the adiabatic invariant, that become larger when ε increases, are very well reproduced by Algorithms 2.1, 2.3 and 2.6.

3.5 Numerical integration of the fast problem

The results presented so far have been obtained with Algorithms 2.1 and 2.3, which require the computation of the matrices $\sin(h\Omega_\varepsilon(q_1))$ and $\cos(h\Omega_\varepsilon(q_1))$. If this computation is too expensive, an alternative is to use Algorithms 2.2 and 2.4. This amounts to numerically (as opposed to exactly) integrating the fast problem (42). We study here the specific impact of such a numerical approximation.

As in Section 3.3, we set $\varepsilon = 10^{-3}$ and monitor the preservation of the energy and of the adiabatic invariant (see estimators (59) and (60)) as a function of h, for different values of the time step h_μ used in the innerloop.

On Figure 9, we compare Algorithms 2.1 and 2.2. As h_μ increases, the accuracy in energy preservation decreases. For a given h_μ, there is a threshold for h below which the accuracy remains constant. We have checked that, when the time step h is in the regime $h \geq \varepsilon\pi$, Algorithm 2.2 with the small value $h_\mu = \varepsilon/(100\Omega)$ gives the same results as Algorithm 2.1.

On Figure 10, we compare Algorithms 2.3 and 2.4. The same conclusions hold as for Algorithms 2.1 and 2.2. On the same figure, we also plot results obtained with Algorithm 2.6. They are very close to those obtained with Algorithm 2.3.

4 Non constant fast frequency

We now consider the case when the fast frequency $\Omega(q_1)$ actually depends on q_1. In Section 4.1, we derive an efficient symplectic algorithm. For brevity, we focus on the differences between the present case and the case of a constant frequency. We report on numerical tests in Section 4.2.

At the beginning of Section 2, we have underlined that several variants are possible in the case of a constant frequency. We have followed some of them in Section 2. In this section, we only follow *one* of such strategies, namely that of Section 2.1 (that is, we work with the original variables). It is not yet clear to us whether the other strategies of Section 2 can be adapted to the present setting.

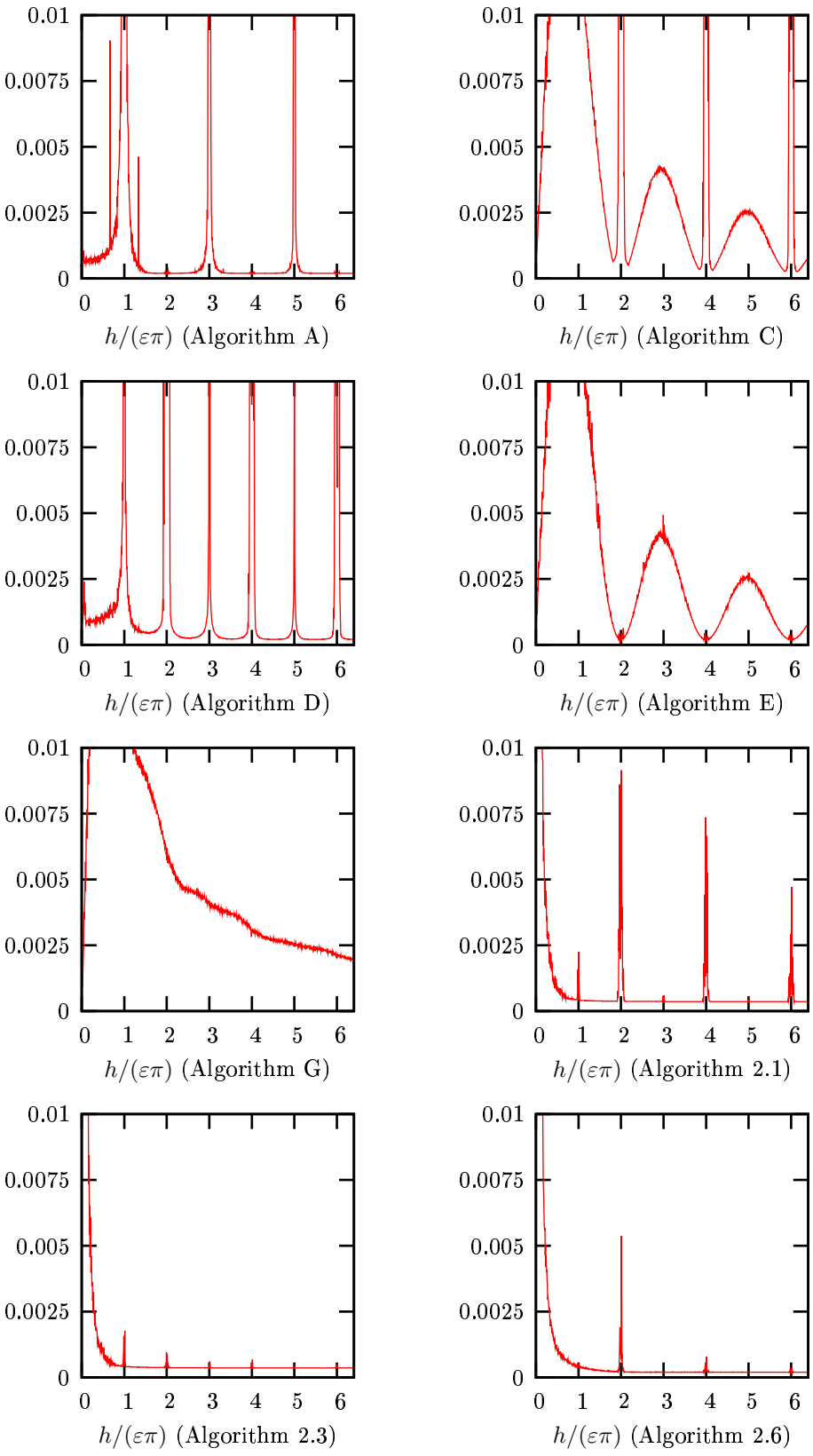

Figure 7: Maximum relative variation (59) of the energy on the time interval $[0, 10^4]$, for several ε ($h = 0.02$). See Table 1 for exponential algorithms terminology.

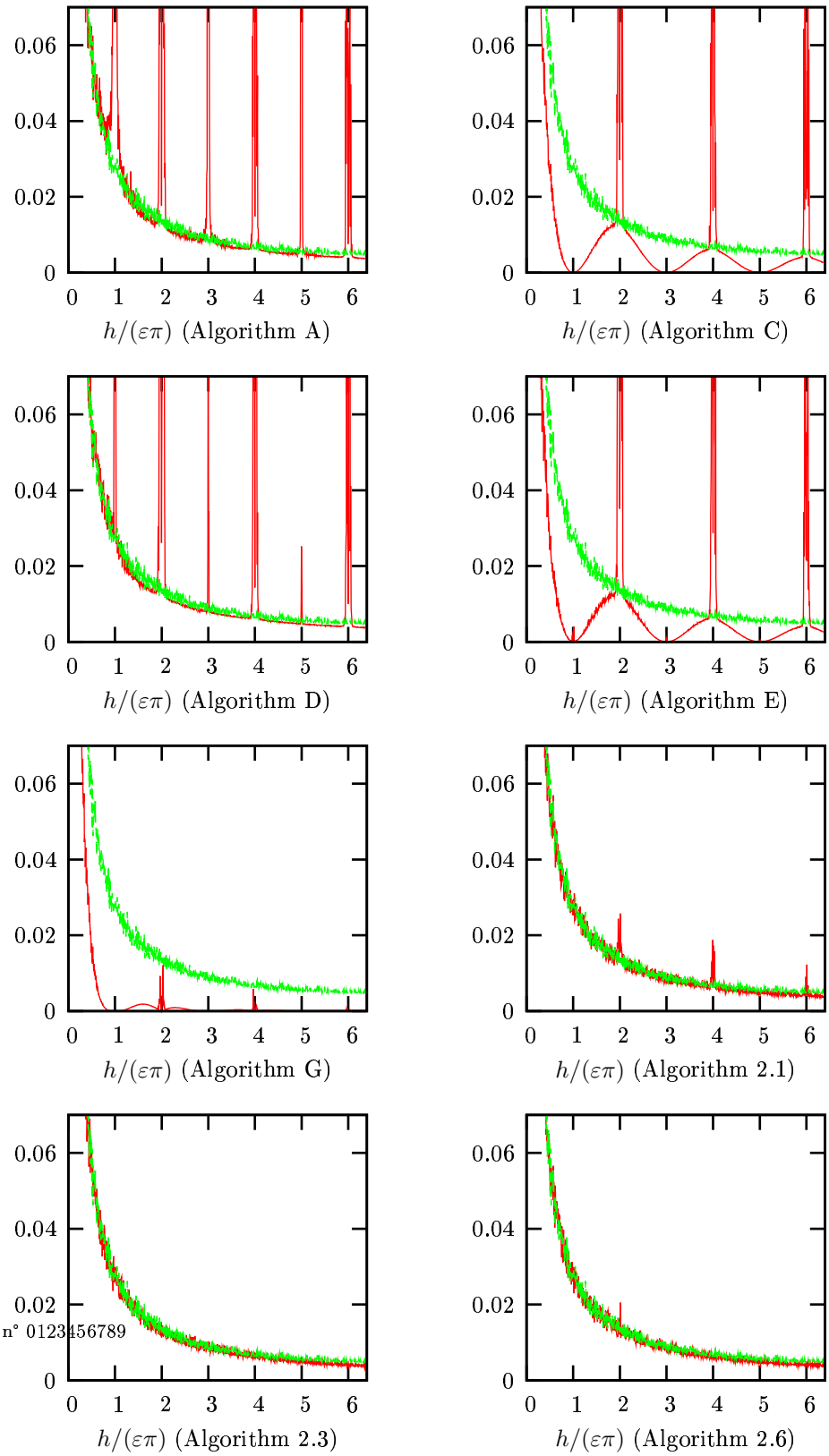

Figure 8: Maximum variation (60) of the adiabatic invariant on the time interval $[0, 10^4]$, for several ε ($h = 0.02$). We compare the numerical results (red curve) with the exact result (green curve). See Table 1 for exponential algorithms terminology.

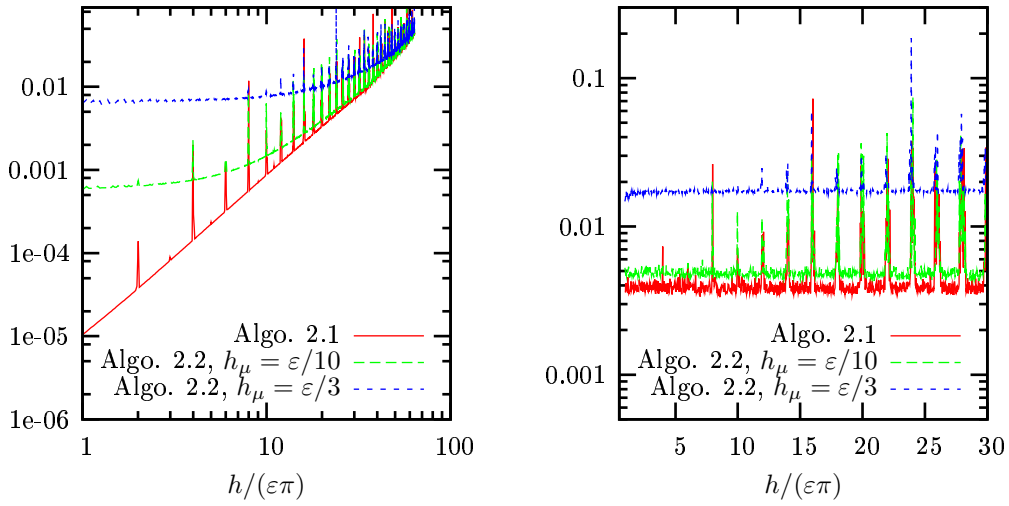

Figure 9: Maximum variation (59) of the energy (left) and maximum variation (60) of the adiabatic invariant (right) on the time interval $[0, 10^4]$ ($\varepsilon = 10^{-3}$), for Algorithms 2.1 and 2.2.

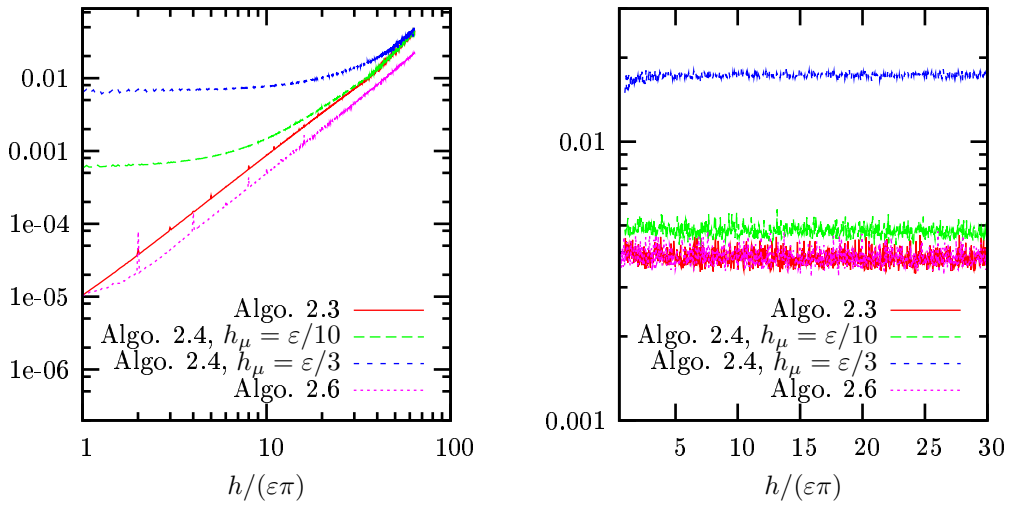

Figure 10: Maximum variation (59) of the energy (left) and maximum variation (60) of the adiabatic invariant (right) on the time interval $[0, 10^4]$ ($\varepsilon = 10^{-3}$), for Algorithms 2.3, 2.4 and 2.6.

4.1 Derivation of a symplectic algorithm

We consider the following Ansatz

$$S_\varepsilon(t,q_1,r_2,P_1,P_2) = S_0(t,q_1,P_1) + \sum_{k\geq 1} \varepsilon^k S_k\left(t, \frac{T(t,q_1,P_1)}{\varepsilon}, q_1, r_2, P_1, P_2\right) \tag{62}$$

for the solution to (6)-(7), where $(S_k)_{k\geq 1}$ are 2π periodic functions in the fast time $\tau = T(t,q_1,P_1)/\varepsilon$. The fast time is chosen such that $\partial_t T = \Omega(q_1(t))$, hence

$$T = \int_0^t \Omega(q_1(s))\, ds.$$

We need to approximate this equation so that T only depends on t, q_1 and P_1. A trapezoidal approximation reads

$$\begin{aligned} T(t) &= \frac{t}{2}\left[\Omega(q_1(0)) + \Omega(q_1(t))\right] + O(t^3) \\ &= \frac{t}{2}\left[\Omega(q_1(0)) + \Omega\left(q_1(0) + \frac{\partial S_0}{\partial P_1}\right)\right] + O(t^3) + O(\varepsilon t) \\ &= \frac{t}{2}\left[\Omega(q_1) + \Omega\left(q_1 + t\frac{\partial^2 S_0}{\partial P_1 \partial t}(t=0)\right)\right] + O(t^3) + O(\varepsilon t). \end{aligned}$$

We set

$$\tau = \frac{T(t,q_1,P_1)}{\varepsilon} := \frac{t}{2\varepsilon}\left[\Omega(q_1) + \Omega\left(q_1 + t\frac{\partial^2 S_0}{\partial P_1 \partial t}(t=0)\right)\right], \tag{63}$$

which is an approximation of order $O(t^3/\varepsilon) + O(t)$ of the exact phase. Thus, if $t \ll \varepsilon^{1/3}$, then τ is a good approximation of the exact phase.

We now insert (62) in (6)-(7), and compare like-powers of ε. The equation of order ε^0 reads

$$\partial_t S_0 + \frac{\partial T}{\partial t}\partial_\tau S_1 = \frac{P_1^T P_1}{2} + \frac{P_2^T P_2}{2} + V_0(q_1 + \partial_{P_1} S_0, 0) + \frac{1}{2}\Omega(q_1 + \partial_{P_1} S_0)^2 \left(\frac{r_2}{\Omega(q_1)} + \partial_{P_2} S_1\right)^2. \tag{64}$$

We now expand this equation in powers of t. The equation of order $\varepsilon^0 t^0$ reads

$$\partial_t S_0 + \frac{\partial T}{\partial t}(t=0)\partial_\tau S_1 = \frac{P_1^T P_1}{2} + \frac{P_2^T P_2}{2} + V_0(q_1,0) + \frac{1}{2}\Omega(q_1)\left(\frac{r_2}{\Omega(q_1)} + \partial_{P_2} S_1\right)^2. \tag{65}$$

Since $\dfrac{\partial T}{\partial t}(t=0) = \Omega(q_1)$, the previous equation can be recast as (15), with Ω replaced by $\Omega(q_1)$. Following the same strategy as in the constant frequency case, we obtain (compare

with (19), (20), (21) and (23))

$$
\begin{aligned}
S_0(t=0) &= 0, && (66)\\
\partial_t S_0(t=0) &= \frac{P_1^T P_1}{2} + V_0(q_1,0), && (67)\\
S_1(t=0) &= \frac{1}{\Omega(q_1)}\left(\frac{P_2^T P_2 + r_2^T r_2}{2}\right)\tan\tau + \frac{P_2^T r_2}{\Omega(q_1)}\left(\frac{1}{\cos\tau} - 1\right), && (68)\\
\frac{\partial^2 S_0}{\partial t^2}(t=0) &= P_1^T \nabla_1 V_0(q_1,0), && (69)\\
\partial_t S_1(t=0) &= -\frac{P_1^T \nabla\Omega(q_1)}{\Omega^2(q_1)}\left(\frac{r_2^T P_2}{2\cos\tau} + \frac{P_2^T P_2 \tan\tau}{2}\right), && (70)
\end{aligned}
$$

where all the functions S_k and their derivatives are evaluated at $(t=0,\tau,q_1,r_2,P_1,P_2)$.

We first consider the approximation $S_\varepsilon(h) \approx \widetilde{S_\varepsilon}(h)$, with

$$
\boxed{\widetilde{S_\varepsilon}(h) := S_0 + h\partial_t S_0 + \varepsilon S_1 + \varepsilon h \partial_t S_1.} \qquad (71)
$$

The scheme on the fast variables is obtained from (5), and reads

$$
\begin{aligned}
P_2 &= \frac{(\cos\tau)p_2 - (\sin\tau)r_2}{1-\beta/2}, && (72)\\
Q_2 &= \frac{\varepsilon}{\Omega}\tan\tau\,(1-\beta)\,P_2 + \frac{1}{\cos\tau}\left(1-\frac{\beta}{2}\right)q_2, && (73)
\end{aligned}
$$

with

$$
\beta = \frac{h}{\Omega(q_1)} P_1^T \nabla\Omega(q_1).
$$

When $\cos\tau \to 0$ and $\sin\tau \to 1$, we can approximate (73) by

$$
Q_2 \approx \frac{1}{(\cos\tau)(1-\beta/2)}\,\frac{\beta^2}{4}\,q_2.
$$

So the scheme is singular in the limit $\cos\tau \to 0$. To remove this singularity, we proceed as in Section 2.1, and now slightly modify the generating function. We have

$$
\begin{aligned}
\widetilde{S_\varepsilon}(h) &= h\left(\frac{1}{2}P_1^T P_1 + V_0(q_1,0)\right)\\
&+ \frac{\varepsilon}{\Omega(q_1)}\left[\frac{r_2^T r_2}{2}\tan\tau + \frac{P_2^T P_2}{2}(1-\beta)\tan\tau - r_2^T P_2 + \frac{r_2^T P_2}{\cos\tau}\left(1-\frac{\beta}{2}\right)\right],
\end{aligned}
$$

that we replace by

$$
\boxed{\begin{aligned}
S_\varepsilon^{\mathrm{NC}}(h) := {} & h\left(\frac{1}{2}P_1^T P_1 + V_0(q_1,0)\right) + \frac{\varepsilon}{\Omega(q_1)}\left[\frac{r_2^T r_2}{2}\tan\tau\right.\\
& \left. + \frac{P_2^T P_2}{2}\exp(-\beta)\tan\tau - r_2^T P_2 + \frac{r_2^T P_2}{\cos\tau}\exp(-\beta/2)\right].
\end{aligned}} \qquad (74)
$$

The difference between (74) and (71) is of order $O(h^2\varepsilon)$, so the order of the approximation has not been modified.

In view of (63) and (67), the fast time τ reads

$$\tau = \frac{h}{2\varepsilon}\left[\Omega(q_1) + \Omega(q_1 + hP_1)\right]. \tag{75}$$

We now insert $S_\varepsilon^{\mathrm{NC}}(h)$ into (5), and obtain the scheme Ψ_h^{NC} (see Algorithm 4.1), which is well defined even in the limit $\cos\tau \to 0$ (see in particular Steps 4 and 5 of the algorithm, that replace (72) and (73)). This scheme is symplectic. The new momentum P_1 is implicitly defined (see Step 2 of the algorithm; note in particular that the fast time τ depends on P_1, see (75)). Once P_1 is determined, the other variables Q_1, Q_2 and P_2 can be computed in an explicit fashion. Computing P_1 amounts to solving a nonlinear equation of the form $\mathcal{F}(P_1) = 0$. To this end, we use a Newton algorithm, and compute the derivative of $\mathcal{F}$ with a finite difference scheme. On the test case reported below, only three iterations were sufficient to converge.

Algorithm 4.1 (Symplectic Scheme $\Psi_h^{\rm NC}(q_1,q_2,p_1,p_2)$)
Set $(q_1,q_2,p_1,p_2)=(q_1^n,q_2^n,p_1^n,p_2^n)$ and perform the following steps:

1. *Set* $r_2 = \dfrac{\Omega(q_1)}{\varepsilon} q_2$.

2. *Solve for P_1 the following implicit equation:*

$$\begin{aligned} p_1 &= P_1 + h\nabla_1 V_0(q_1,0) \\ &- \frac{\varepsilon}{\Omega^2(q_1)}\left(p_2^T r_2 \sin^2\tau^* + \frac{r_2^T r_2 - p_2^T p_2}{2}\ \sin\tau^*\cos\tau^*\right)\nabla\Omega(q_1) \\ &+ \frac{h}{4\Omega(q_1)}\left(r_2^T r_2 + p_2^T p_2\right)\left(\nabla\Omega(q_1)+\nabla\Omega(q_1+hP_1)\right) \\ &- \frac{h\varepsilon}{\Omega(q_1)}\left(\frac{p_2^T p_2 - r_2^T r_2}{2}\ \sin\tau^*\cos\tau^* + p_2^T r_2\left(\frac{1}{2}-\sin^2\tau^*\right)\right) d(q_1,P_1), \end{aligned}$$

with $\tau^* = \dfrac{h}{2\varepsilon}\left[\Omega(q_1)+\Omega(q_1+hP_1)\right]$ *and* $d(q_1,P_1) = \nabla_{q_1}\left(\dfrac{P_1^T\nabla\Omega(q_1)}{\Omega(q_1)}\right)$.

3. *Set* $\tau = \dfrac{h}{2\varepsilon}\left[\Omega(q_1)+\Omega(q_1+hP_1)\right]$ *and* $\beta = \dfrac{h}{\Omega(q_1)} P_1^T\nabla\Omega(q_1)$.

4. *Set* $P_2 = \exp(\beta/2)\left((\cos\tau)p_2 - (\sin\tau)r_2\right)$.

5. *Set* $Q_2 = \exp(-\beta/2)\left((\cos\tau)q_2 + \dfrac{\varepsilon\sin\tau}{\Omega(q_1)}p_2\right)$.

6. *Set*

$$\begin{aligned} Q_1 &= q_1 + hP_1 + \frac{h^2}{4\Omega(q_1)}\left(r_2^T r_2 + p_2^T p_2\right)\nabla\Omega(q_1+hP_1) \\ &- \frac{h\varepsilon}{\Omega^2(q_1)}\left(\frac{p_2^T p_2 - r_2^T r_2}{2}\ \sin\tau\cos\tau + p_2^T r_2\left(\frac{1}{2}-\sin^2\tau\right)\right)\nabla\Omega(q_1). \end{aligned}$$

Set $\left(q_1^{n+1},q_2^{n+1},p_1^{n+1},p_2^{n+1}\right) = (Q_1,Q_2,P_1,P_2)$.

Remark 8 *It is shown in [3, 4] in the case of scalar fast variables ($q_2\in\mathbb{R}$, $p_2\in\mathbb{R}$) that the dynamics on the slow variables obtained in the limit $\varepsilon\to 0$ is a dynamics of hamiltonian* $H_1^{\rm NC} = \dfrac{p_1^T p_1}{2} + V_0(q_1,0) + C\Omega(q_1)$, *where*

$$C = \lim_{\varepsilon\to 0}\ \frac{p_2^2(0) + \Omega^2(q_1(0))\ q_2^2(0)/(\varepsilon^2)}{2\Omega(q_1(0))}$$

is a constant which depends on the initial conditions. We show in this remark that, in the limit $\varepsilon \to 0$, Algorithm 4.1 is consistent with this theoretical result.

We first check that, for the slow variables, in the limit $\varepsilon \to 0$, Algorithm 4.1 is the symplectic algorithm which is derived from the generating function

$$S^{\rm NC}_{\rm num}(h, q_1, P_1) = h\left(V_0(q_1, 0) + \frac{P_1^T P_1}{2} + \frac{C}{2}\left[\Omega(q_1) + \Omega(q_1 + hP_1)\right]\right),$$

where $C = \dfrac{p_2^T p_2 + \Omega^2(q_1)\ q_2^T q_2/(\varepsilon^2)}{2\Omega(q_1)}$ *is supposed to be a constant. We observe that*

$$S^{\rm NC}_{\rm num}(h, q_1, P_1) = S^{\rm NC}(h, q_1, P_1) + O(h^2),$$

where $S^{\rm NC}(t, q_1, P_1)$ is the solution of the Hamilton-Jacobi equation associated to $H_1^{\rm NC}$.

Additionally, the time step h being fixed, we check on Algorithm 4.1 that

$$\lim_{\varepsilon \to 0} \frac{P_2^T P_2 + \Omega^2(Q_1)\ Q_2^T Q_2/(\varepsilon^2)}{p_2^T p_2 + \Omega^2(q_1)\ q_2^T q_2/(\varepsilon^2)}\ \frac{\Omega(q_1)}{\Omega(Q_1)} = 1 + O(h^2).$$

Up to the term $O(h^2)$, this is consistent with the fact that $\dfrac{1}{\Omega(q_1)}\left(\dfrac{p_2^T p_2}{2} + \Omega^2(q_1)\ \dfrac{q_2^T q_2}{2\varepsilon^2}\right)$ *is an adiabatic invariant of the dynamics (see [3, 4]).*

4.2 Numerical results

We have implemented Algorithm 4.1 in the scalar case ($q_1 \in \mathbb{R}$, $q_2 \in \mathbb{R}$), with

$$\Omega(q_1) = \sqrt{1 + q_1^2} \quad \text{and} \quad V_0(q_1, q_2) = (q_1^2 + q_2^2 - 1)^2.$$

In addition to the preservation of energy, we will monitor the variation of

$$I = \frac{\dfrac{p_2^2}{2} + \Omega(q_1)^2 \dfrac{q_2^2}{2\varepsilon^2}}{\Omega(q_1)} \tag{76}$$

along the trajectory. Recall that I is an adiabatic invariant (see [3, 4]), and that, for a given time frame, its variation decreases as ε decreases.

We first choose $\varepsilon = 10^{-3}$ and $h = 0.02$, and monitor the evolution of the energy and adiabatic invariant up to time $T = 10^5$. Results are shown on Figure 11. No drift can be seen.

We now study the robustness of the algorithm. We set the time step to $h = 0.02$, and consider the variation of the energy (see estimator (59)) and the variation of the adiabatic invariant (76) (see estimator (60)), over the time frame $t \in [0, 10^5]$, for stiffness ε varying between 10^{-3} to 1. Results are shown on Figure 12. We do not observe decreasing performances of the algorithm as ε decreases.

On Figure 13, we plot the global errors (61) at time $T = 1$ of q_1, q_2/ε, p_1 and p_2. We observe a very good accuracy, even if $h \gg \varepsilon$.

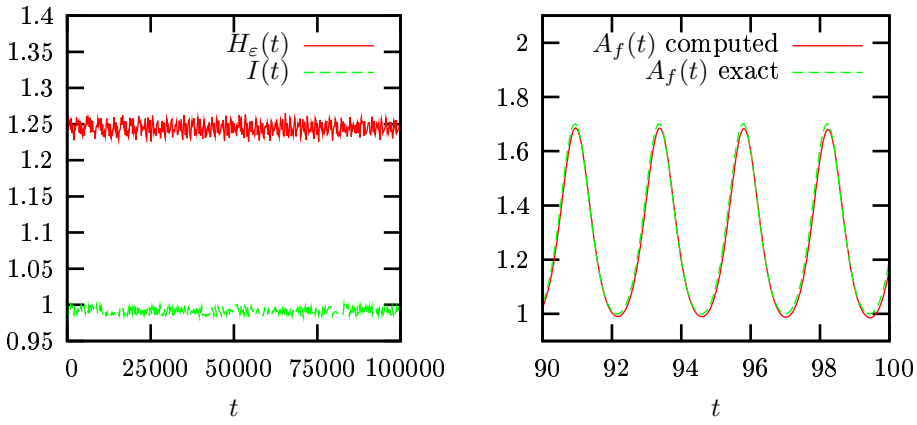

Figure 11: Left: Energy and adiabatic invariant along the trajectory ($\varepsilon = 10^{-3}$ and $h = 0.02$). Right: as expected, $A_f = \frac{p_2^2}{2} + (\Omega(q_1))^2 \, \frac{q_2^2}{2\varepsilon^2}$ varies.

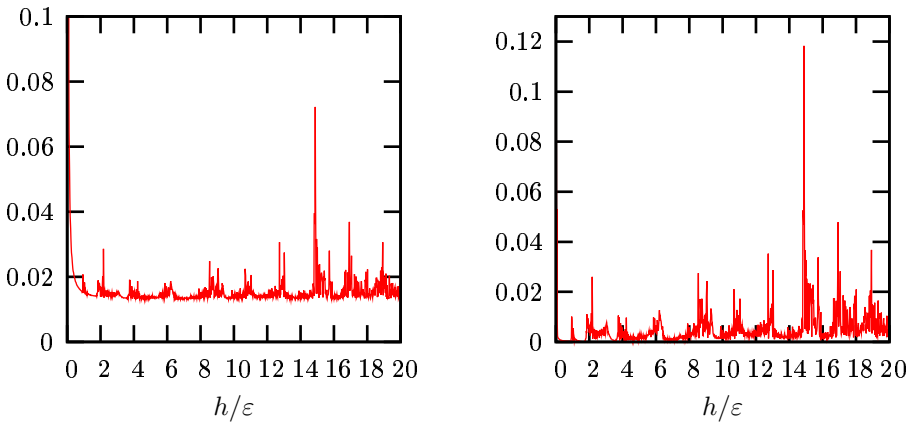

Figure 12: Maximum variation (59) of the energy (left) and maximum variation (60) of the adiabatic invariant (right) on the time interval $[0, 10^5]$, for several ε ($h = 0.02$), for Algorithm 4.1.

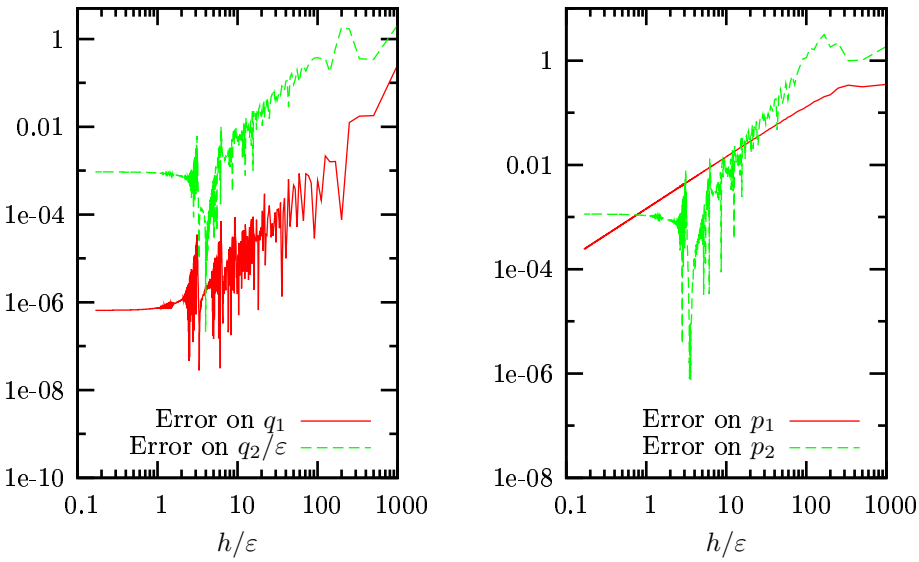

Figure 13: Global errors (61) at time $T = 1$, for several time steps h ($\varepsilon = 10^{-3}$).

References

[1] G. Benettin, A. Giorgilli, On the Hamiltonian interpolation of near to the identity symplectic mappings with application to symplectic integration algorithms, J. Stat. Phys. 74 (1994) 1117–1143.

[2] J.J. Biesiadecki, R.D. Skeel, Dangers of multiple time step methods, J. Comput. Phys. 109 (1993) 318–328.

[3] F. Bornemann, Homogenization in time of singularly perturbed mechanical systems, Lectures Notes in Mathematics 1687, Springer, 1998.

[4] F. Bornemann, Ch. Schuette, Homogenization of hamiltonian systems with a strong constraining potential, Physica D 102 (1997) 57–77.

[5] F. Castella, Ph. Chartier, E. Faou, work in progress.

[6] D. Cohen, E. Hairer, Ch. Lubich, Modulated Fourier Expansions of highly oscillatory differential equations, Found. Comput. Math. 3 (2003) 327–345.

[7] D. Cohen, E. Hairer, Ch. Lubich, Numerical energy conservation for multi-frequency oscillatory differential equations, BIT 45 (2005) 287–305.

[8] D. Cohen, T. Jahnke, K. Lorenz and Ch. Lubich, Numerical integrators for highly oscillatory Hamiltonian systems: a review, preprint available at http://na.uni-tuebingen.de/articles.shtml.

[9] P. Deuflhard, A study of extrapolation methods based on multistep schemes without parasitic solutions, Z. Angew. Math. Phys. 30 (1979) 177–189.

[10] B. Engquist, R. Tsai, Heterogeneous multiscale methods for stiff ordinary differential equations, Math. Comput. 74(252) (2005) 1707–1742.

[11] E. Faou, E. Hairer, T.-L. Pham, Energy conservation with non-symplectic methods: examples and counter-examples, BIT 44 (2004) 699–709.

[12] K. Feng, Difference schemes for Hamiltonian formalism and symplectic geometry, J. Comp. Math. 4 (1986) 279–289.

[13] B. Garcia-Archilla, J.M. Sanz-Serna, R.D. Skeel, Long time step methods for oscillatory differential equations, SIAM J. Sci. Comput. 20(3) (1998) 930–963.

[14] W. Gautschi, Numerical integration of ordinary differential equations based on trigonometric polynomials, Numer. Math. 3 (1961) 381–397.

[15] V. Grimm, M. Hochbruck, Error analysis of exponential integrators for oscillatory second-order differential equations, J. Phys. A 39 (2006) 5495–5507.

[16] H. Grubmüller, H. Heller, A. Windemuth, K. Schulten, Generalized Verlet algorithm for efficient molecular dynamics simulations with long range interaction, Mol. Sim. 6(1-3) (1991) 121–142.

[17] E. Hairer, Long time energy conservation of numerical integrators, Foundations of Computational Mathematics, Santander 2005, London Math. Soc. Lecture Notes 331, Cambridge University Press (2006) 162–180.

[18] E. Hairer, Ch. Lubich, The life-span of backward error analysis for numerical integrators, Numer. Math. 76 (1997) 441–462, erratum http://www.unige.ch/math/folks/hairer

[19] E. Hairer, Ch. Lubich, Energy conservation by Störmer-type numerical integrators, in G.F. Griffiths, G.A. Watson eds, Numerical Analysis 1999, CRC Press LLC, 169–190.

[20] E. Hairer, Ch. Lubich, Long-time energy conservation of numerical methods for oscillatory differential equations, SIAM J. Numer. Anal. 38 (2000) 414–441.

[21] E. Hairer, Ch. Lubich, G. Wanner, Geometric Numerical Integration, Springer, 2006.

[22] M. Hochbruck, Ch. Lubich, A Gautschi-type method for oscillatory second-order differential equations, Numer. Math. 83 (1999) 403–426.

[23] A. Iserles, On the global error of discretization methods for highly-oscillatory ordinary differential equations, BIT 42 (2002) 561–599.

[24] J.A. Izaguirre, S. Reich, R.D. Skeel, Longer time steps for Molecular Dynamics, J. Chem. Phys. 110(20) (1999) 9853–9864.

[25] T. Jahnke, Long-time-step integrators for almost-adiabatic quantum dynamics, SIAM J. Sci. Comput. 25 (2004) 2145–2164.

[26] T. Jahnke, Ch. Lubich, Numerical integrators for quantum dynamics close to to the adiabatic limit, Numer. Math. 94 (2003) 289–314.

[27] Z. Jia, B. Leimkuhler, Geometric integrators for multiple time-scale simulation, J. Phys. A 39 (2006) 5379–5403.

[28] C. Le Bris, F. Legoll, Dérivation de schémas numériques symplectiques pour des systèmes hamiltoniens hautement oscillants (Derivation of symplectic numerical schemes for highly oscillatory Hamiltonian systems), C. R. Acad. Sci. Paris, Série I, vol. 344(4) (2007) 277–282.

[29] B.J. Leimkuhler, S. Reich, A reversible averaging integrator for multiple time-scale dynamics, J. Comput. Phys. 171 (2001) 95–114.

[30] K. Lorenz, T. Jahnke and Ch. Lubich, Adiabatic integrators for highly oscillatory second order linear differential equations with time-varying eigendecomposition, BIT 45 (2005) 91–115.

[31] S. Reich, Backward error analysis for numerical integrators, SIAM J. Numer. Anal. 36 (1999) 1549–1570.

[32] S. Reich, Smoothed Langevin dynamics of highly oscillatory systems, Physica D 138 (2000) 210–224.

[33] J.M. Sanz-Serna, work in preparation.

[34] R. Sharp, R. Tsai, B. Engquist, Multiple time scale numerical methods for the inverted pendulum problem, in Lectures Notes in Computational Science and Engineering 44, Springer (2005) 241–261.

[35] M.E. Tuckermann, B.J. Berne, G.J. Martyna, Reversible multiple time scale molecular dynamics, J. Chem. Phys. 97 (1992) 1990–2001.

5 Appendix: the direct approach in the case of a constant fast frequency

In this Appendix, we compute the expansion with respect to ε and t that comes from the insertion of (8) in (6)-(7), and we identify like-powers in ε and t. We recall that the equations of order ε^0 and ε are respectively (13) and (14). The final outcome of this identification procedure is system (21)-(25).

5.1 The equation of order $\varepsilon^0 t$

We consider the equation of order $\varepsilon^0 t$ that comes from (13). Making use of (19) and (20), it reads

$$\partial_{tt} S_0(t=0) + \Omega \partial_{t\tau} S_1(t=0) = P_1^T \nabla_1 V_0(q_1,0) + \Big(\frac{r_2}{\cos\tau} + (\tan\tau) P_2\Big)^T \Omega \partial_{tP_2} S_1(t=0). \quad (77)$$

We recognize here a transport equation on $\Omega \partial_t S_1(t=0)$, in the variables (τ, P_2). Let us solve this equation by the method of characteristics. We thus consider the ODE

$$\frac{d\Phi}{d\tau} = -\frac{r_2}{\cos\tau} - (\tan\tau)\Phi, \quad \Phi(\tau=0) = P_2, \quad (78)$$

whose solution is parametrized by r_2 and P_2 and reads $\Phi(\tau, r_2, P_2) = (\cos\tau) P_2 - (\sin\tau) r_2$. We thus introduce the function

$$B(\tau, q_1, r_2, P_1, P_2) = \Omega \partial_t S_1(t=0, \tau, q_1, r_2, P_1, \Phi(\tau, r_2, P_2)). \quad (79)$$

In view of (77), this function satisfies

$$\partial_\tau B = P_1^T \nabla_1 V_0(q_1,0) - \partial_{tt} S_0(t=0).$$

We observe that the right hand side of the above equation does not depend on τ. On the other hand, Φ and $\partial_t S_1(t=0)$ are 2π periodic in τ, hence B is also 2π periodic in τ, by its definition (79). We thus obtain that $\partial_\tau B = 0$, and hence

$$\partial_{tt} S_0(t=0) = P_1^T \nabla_1 V_0(q_1,0), \quad (80)$$

$$\partial_t S_1(t=0, \tau, q_1, r_2, P_1, \Phi(\tau, r_2, P_2)) \text{ does not depend on } \tau. \quad (81)$$

5.2 The equation of order εt^0

We now consider the equation of order εt^0 that comes from (14). It reads

$$\partial_t S_1 + \Omega \partial_\tau S_2 = \Omega \Big(\frac{r_2}{\cos\tau} + (\tan\tau) P_2\Big)^T \partial_{P_2} S_2 \; + \; \frac{1}{\Omega} (\nabla_2 V_0)^T \Big(\frac{r_2}{\cos\tau} + (\tan\tau) P_2\Big).$$

We again recognize a transport equation, on the function $\Omega S_2(t=0)$, in the variables (τ, P_2). We thus introduce the function

$$C(\tau, q_1, r_2, P_1, P_2) = \Omega S_2(t=0, \tau, q_1, r_2, P_1, \Phi(\tau, r_2, P_2)), \tag{82}$$

with Φ the solution to (78). The function C satisfies

$$\partial_\tau C = \frac{1}{\Omega}(\nabla_2 V_0)^T \left((\cos\tau) r_2 + (\sin\tau) P_2\right) - \partial_t S_1(t=0, \tau, q_1, r_2, P_1, \Phi(\tau, r_2, P_2)). \tag{83}$$

In view of its definition, the function C is 2π periodic in τ. We integrate the above equation from 0 to 2π and obtain

$$\int_0^{2\pi} \partial_t S_1(t=0, \tau, q_1, r_2, P_1, \Phi(\tau, r_2, P_2))\, d\tau = 0.$$

We know with (81) that $\partial_t S_1(t=0, \tau, q_1, r_2, P_1, \Phi(\tau, r_2, P_2))$ actually does not depend on τ. We thus obtain

$$\partial_t S_1(t=0, \tau, q_1, r_2, P_1, P_2) = 0 \tag{84}$$

for all $(\tau, q_1, r_2, P_1, P_2)$. Thus (83) actually reads

$$\partial_\tau C = \frac{1}{\Omega}(\nabla_2 V_0)^T \left((\cos\tau) r_2 + (\sin\tau) P_2\right).$$

We now integrate this equation with respect to τ. With the initial condition $C(\tau=0)=0$, which comes from $S_2(t=\tau=0)=0$, we obtain the expression of $C(\tau)$ for all τ, and thus, in view of (82), the following expression for S_2:

$$S_2(t=0, \tau, q_1, r_2, P_1, P_2) = \frac{1}{\Omega^2}(\nabla_2 V_0(q_1, 0))^T \left(\frac{P_2}{\cos\tau} - P_2 + (\tan\tau) r_2\right). \tag{85}$$

5.3 The equation of order $\varepsilon^0 t^2$

We now look for the expression of $\partial_t S_2$. We note that, to get the expression of S_2, we have made use of the equations of order εt^0 and $\varepsilon^0 t$. In order to get the expression for $\partial_t S_2$, we will need the equation of order $\varepsilon^2 t^0$, εt and $\varepsilon^0 t^2$.

The equation of order $\varepsilon^0 t^2$ reads

$$\begin{aligned} \partial_{ttt} S_0(t=0) \quad &+ \quad \Omega \partial_{tt\tau} S_1(t=0) \\ &= \quad (\nabla_1 V_0(q_1, 0))^T \nabla_1 V_0(q_1, 0) + P_1^T \nabla_{11} V_0(q_1, 0) P_1 \\ &+ \quad \left(\frac{r_2}{\cos\tau} + (\tan\tau) P_2\right)^T \Omega \partial_{ttP_2} S_1(t=0). \end{aligned}$$

As we have done it previously, we introduce the intermediate function

$$D(\tau, q_1, r_2, P_1, P_2) = \Omega \partial_{tt} S_1(t=0, \tau, q_1, r_2, P_1, \Phi(\tau, r_2, P_2)),$$

which satisfies the equation

$$\partial_{ttt} S_0(t=0) + \partial_\tau D = (\nabla_1 V_0(q_1,0))^T \nabla_1 V_0(q_1,0) + P_1^T \nabla_{11} V_0(q_1,0) P_1.$$

The function D is periodic in τ and S_0 does not depend on τ, so $\partial_\tau D = 0$, hence

$$\partial_{ttt} S_0(t=0) = (\nabla_1 V_0(q_1,0))^T \nabla_1 V_0(q_1,0) + P_1^T \nabla_{11} V_0(q_1,0) P_1, \tag{86}$$

$$\partial_{tt} S_1(t=0,\tau,q_1,r_2,P_1,\Phi(\tau,r_2,P_2)) \quad \text{does not depend on} \quad \tau. \tag{87}$$

5.4 The equation of order εt

We now write the equation of order εt. This is again a transport equation, so we introduce

$$E(\tau,q_1,r_2,P_1,P_2) = \Omega \partial_t S_2(t=0,\tau,q_1,r_2,P_1,\Phi(\tau,r_2,P_2)),$$

which satisfies

$$\partial_{tt} S_1(t=0,\tau,q_1,r_2,P_1,\Phi(\tau,r_2,P_2)) + \partial_\tau E = \frac{1}{\Omega} P_1^T \nabla_{12} V_0(q_1,0)((\sin\tau)P_2 + (\cos\tau) r_2). \tag{88}$$

The function E is 2π periodic in τ, so

$$\int_0^{2\pi} \partial_{tt} S_1(t=0,\tau,q_1,r_2,P_1,\Phi(\tau,r_2,P_2))\, d\tau = 0.$$

In view of (87), we obtain

$$\partial_{tt} S_1(t=0,\tau,q_1,r_2,P_1,P_2) = 0. \tag{89}$$

We can thus integrate the equation (88) and we obtain the expression of $E(\tau)$ for all τ. This gives the following expression for $\partial_t S_2$:

$$\begin{aligned} \partial_t S_2(t=0,\tau,q_1,r_2,P_1,\Phi(\tau,r_2,P_2)) &= \partial_t S_2(t=0,\tau=0,q_1,r_2,P_1,P_2) \\ &+ \frac{1}{\Omega^2} P_1^T \nabla_{12} V_0(q_1,0)(P_2 - (\cos\tau)P_2 + (\sin\tau) r_2). \end{aligned} \tag{90}$$

5.5 The equation of order $\varepsilon^2 t^0$

We now write the equation of order $\varepsilon^2 t^0$. It reads

$$\begin{aligned} \partial_t S_2(t=0) &+ \Omega \partial_\tau S_3(t=0) \\ &= \frac{1}{2\Omega^2}\left(\frac{1}{\cos\tau} - 1\right)^2 (\nabla_2 V_0(q_1,0))^2 + \frac{1}{\Omega^2}\left(\frac{1}{\cos\tau} - 1\right)(\nabla_2 V_0(q_1,0))^2 \\ &+ \left(\frac{r_2}{\cos\tau} + (\tan\tau)P_2\right)^T \Omega \partial_{P_2} S_3(t=0) \\ &+ \frac{1}{2\Omega^2}\left(\frac{r_2}{\cos\tau} + (\tan\tau)P_2\right)^T \nabla_{22} V_0(q_1,0)\left(\frac{r_2}{\cos\tau} + (\tan\tau)P_2\right). \end{aligned}$$

This is a transport equation on $\Omega S_3(t=0)$. We thus introduce

$$F(\tau, q_1, r_2, P_1, P_2) = \Omega S_3(t=0, \tau, q_1, r_2, P_1, \Phi(\tau, r_2, P_2)),$$

which satisfies

$$\begin{aligned}
\partial_t S_2(t &= 0, \tau, q_1, r_2, P_1, \Phi) + \partial_\tau F = \frac{1}{2\Omega^2}\left(\frac{1}{\cos\tau} - 1\right)^2 (\nabla_2 V_0(q_1, 0))^2 \\
&+ \frac{1}{\Omega^2}\left(\frac{1}{\cos\tau} - 1\right)(\nabla_2 V_0(q_1, 0))^2 \\
&+ \frac{1}{2\Omega^2}\left((\cos\tau) r_2 + (\sin\tau) P_2\right)^T \nabla_{22} V_0(q_1, 0)\left((\cos\tau) r_2 + (\sin\tau) P_2\right).
\end{aligned}$$

We integrate the above equation between 0 and 2π and we use the fact that F is 2π periodic:

$$\begin{aligned}
\frac{1}{2\pi}\int_0^{2\pi} \partial_t S_2(t=0, \tau, q_1, r_2, P_1, \Phi)\, d\tau &= \frac{-1}{2\Omega^2}(\nabla_2 V_0(q_1, 0))^2 \\
&+ \frac{1}{4\Omega^2}\left(P_2^T \nabla_{22} V_0(q_1, 0) P_2 + r_2^T \nabla_{22} V_0(q_1, 0) r_2\right).
\end{aligned}$$

We now insert equation (90) in the above equation, and obtain the expression of $\partial_t S_2(t = 0, \tau = 0, q_1, r_2, P_1, P_2)$. In turn, using again (90), we obtain

$$\begin{aligned}
\partial_t S_2(t=0, \tau, q_1, r_2, P_1, P_2) &= \frac{-1}{2\Omega^2}(\nabla_2 V_0(q_1, 0))^2 - \frac{1}{\Omega^2} P_1^T \nabla_{12} V_0(q_1, 0) P_2 \\
+ \frac{1}{4\Omega^2 \cos^2\tau}&\left(P_2^T \nabla_{22} V_0 P_2 + r_2^T \nabla_{22} V_0 r_2 + 2\sin\tau\, r_2^T \nabla_{22} V_0 P_2\right). \qquad (91)
\end{aligned}$$

6 Appendix: preconditionning the dynamics in the case of a constant fast frequency

In this Appendix, we carry out the identification process that results from the insertion of (49) in (48). The final outcome of this procedure are the equations (55) and (56).

We have already worked on the equation of order ε^0 in Section 2.3. We now consider the equation of order ε, which reads

$$\partial_t S_1 + \Omega \partial_\tau S_2 = (\nabla_1 V_0^*)^T \partial_{P_1} S_1 + \frac{1}{\Omega}(\nabla_2 V_0^*)^T \left[\cos\tau\,(r_2 + \Omega \partial_{Y_2} S_1) + (\sin\tau) Y_2\right], \qquad (92)$$

with the notation

$$\nabla_1 V_0^* = \nabla_1 V_0(q_1 + \partial_{P_1} S_0, 0).$$

We now average this equation in $\tau \in [0, 2\pi]$ and make use of (52) and the periodicity of S_2. We obtain

$$\partial_t S_1 = (\nabla_1 V_0^*)^T \partial_{P_1} S_1, \qquad (93)$$

$$\Omega \partial_\tau S_2 = \frac{1}{\Omega}(\nabla_2 V_0^*)^T \left[\cos\tau\,(r_2 + \Omega \partial_{Y_2} S_1) + (\sin\tau) Y_2\right]. \qquad (94)$$

The equation (93) is a transport equation on S_1, in the variables t and P_1. With the initial condition $S_1(t=0)=0$, we obtain

$$S_1(t,q_1,r_2,P_1,Y_2)=0. \tag{95}$$

We insert $S_1 \equiv 0$ in (85) and integrate the equation with respect to τ. We obtain:

$$S_2(\tau)-S_2(\tau=0)=\frac{1}{\Omega^2}(\nabla_2 V_0^*)^T\left((\sin\tau)r_2+(1-\cos\tau)Y_2\right), \tag{96}$$

where $S_2(\tau)$ is a notation for $S_2(t,\tau,q_1,r_2,P_1,Y_2)$. In order to compute an approximation of S_2, we now make the approximation

$$\nabla_2 V_0^* = \nabla_2 V_0\left(q_1+\frac{\partial S_0}{\partial P_1}(t,q_1,P_1),0\right)\approx \nabla_2 V_0^{\rm SE},$$

with

$$\nabla_2 V_0^{\rm SE} = \nabla_2 V_0\left(q_1+\frac{\partial S_0^{\rm SE}}{\partial P_1}(t,q_1,P_1),0\right)=\nabla_2 V_0\left(q_1+tP_1,0\right).$$

We thus approximate S_2 by $S_2^{\rm SE}$ which solves (compare with (96))

$$S_2^{\rm SE}(\tau)-S_2^{\rm SE}(\tau=0)=\frac{1}{\Omega^2}(\nabla_2 V_0^{\rm SE})^T\left((\sin\tau)r_2+(1-\cos\tau)Y_2\right). \tag{97}$$

We now consider the equation of order ε^2 that comes from the expansion of (48). It reads

$$\begin{aligned}\partial_t S_2+\Omega\partial_\tau S_3 &= (\nabla_1 V_0^*)^T\partial_{P_1}S_2 \;+\; (\nabla_2 V_0^*)^T\partial_{Y_2}S_2\;\cos\tau \\ &+ \frac{1}{2\Omega^2}\left((\cos\tau)r_2+(\sin\tau)Y_2\right)^T\nabla_{22}V_0^*\left((\cos\tau)r_2+(\sin\tau)Y_2\right).\end{aligned} \tag{98}$$

As in (96), we approximate S_2 by $S_2^{\rm SE}$, and S_3 by $S_3^{\rm SE}$, such that $S_2^{\rm SE}$ and $S_3^{\rm SE}$ solve (compare with (98))

$$\begin{aligned}\partial_t S_2^{\rm SE}+\Omega\partial_\tau S_3^{\rm SE} &= (\nabla_1 V_0^{\rm SE})^T\partial_{P_1}S_2^{\rm SE} \;+\; (\nabla_2 V_0^{\rm SE})^T\partial_{Y_2}S_2^{\rm SE}\;\cos\tau \\ &+ \frac{1}{2\Omega^2}\left((\cos\tau)r_2+(\sin\tau)Y_2\right)^T\nabla_{22}V_0^{\rm SE}\left((\cos\tau)r_2+(\sin\tau)Y_2\right).\end{aligned} \tag{99}$$

With (97) and (99), we now compute an approximation of $S_2^{\rm SE}$. We first average (99) in $\tau\in[0,2\pi]$. Let us introduce

$$C(t,q_1,r_2,P_1,Y_2)=\frac{1}{2\pi}\int_0^{2\pi} S_2^{\rm SE}(t,\tau,q_1,r_2,P_1,Y_2)\,d\tau.$$

In view of (99), C satisfies the equation

$$\begin{aligned}\partial_t C &= (\nabla_1 V_0^{\rm SE})^T\partial_{P_1}C \;+\; (\nabla_2 V_0^{\rm SE})^T\frac{1}{2\pi}\int_0^{2\pi}\cos\tau\,\frac{\partial S_2^{\rm SE}}{\partial Y_2}(\tau)\,d\tau \\ &+ \frac{1}{4\Omega^2}\left(r_2^T\nabla_{22}V_0^{\rm SE}r_2+Y_2^T\nabla_{22}V_0^{\rm SE}Y_2\right).\end{aligned} \tag{100}$$

We infer from (97) that

$$\frac{\partial S_2^{\rm SE}}{\partial Y_2}(\tau) - \frac{\partial S_2^{\rm SE}}{\partial Y_2}(\tau=0) = \frac{1}{\Omega^2}(1-\cos\tau)\nabla_2 V_0^{\rm SE},$$

so

$$\frac{1}{2\pi}\int_0^{2\pi} \cos\tau \, \frac{\partial S_2^{\rm SE}}{\partial Y_2}(\tau)\, d\tau = -\frac{1}{2\Omega^2}\nabla_2 V_0^{\rm SE},$$

and (100) thus reads

$$\partial_t C = (\nabla_1 V_0^{\rm SE})^T \partial_{P_1} C \; - \; \frac{1}{2\Omega^2}(\nabla_2 V_0^{\rm SE})^T \nabla_2 V_0^{\rm SE} + \frac{1}{4\Omega^2}\left(r_2^T \nabla_{22} V_0^{\rm SE} r_2 + Y_2^T \nabla_{22} V_0^{\rm SE} Y_2\right). \tag{101}$$

The equation (101) is a transport equation on C, which we integrate with the method of characteristics. For any p_1, let us introduce

$$\Phi(t, q_1, p_1) = p_1 - t\nabla_1 V_0(q_1, 0).$$

We set

$$D(t, q_1, r_2, p_1, Y_2) = C(t, q_1, r_2, \Phi(t, q_1, p_1), Y_2),$$

which solves

$$\partial_t D = -\frac{1}{2\Omega^2}(\nabla_2 V_0^\Phi)^T \nabla_2 V_0^\Phi + \frac{1}{4\Omega^2}\left(r_2^T \nabla_{22} V_0^\Phi r_2 + Y_2^T \nabla_{22} V_0^\Phi Y_2\right)$$

with $\nabla_2 V_0^\Phi = \nabla_2 V_0(q_1 + t\Phi(t, q_1, p_1), 0)$. The function $D(t)$ is approximated by

$$\begin{aligned} D(t) &\approx D(t=0) + t\partial_t D(t=0) \\ &= C(0, q_1, r_2, p_1, Y_2) - \frac{t}{2\Omega^2}(\nabla_2 V_0)^T \nabla_2 V_0 + \frac{t}{4\Omega^2}\left(r_2^T \nabla_{22} V_0 r_2 + Y_2^T \nabla_{22} V_0 Y_2\right), \end{aligned}$$

where the derivatives of V_0 are evaluated at $(q_1, 0)$. Hence

$$\begin{aligned} C(t, q_1, r_2, P_1, Y_2) &= C(0, q_1, r_2, P_1 + t\nabla_1 V_0, Y_2) - \frac{t}{2\Omega^2}(\nabla_2 V_0)^T \nabla_2 V_0 \\ &+ \frac{t}{4\Omega^2}\left(r_2^T \nabla_{22} V_0 r_2 + Y_2^T \nabla_{22} V_0 Y_2\right). \end{aligned}$$

We now average out (97) in τ and obtain

$$C(t, q_1, r_2, P_1, Y_2) - S_2^{\rm SE}(t, \tau=0, q_1, r_2, P_1, Y_2) = \frac{1}{\Omega^2}(\nabla_2 V_0^{\rm SE})^T Y_2.$$

Collecting the above two equations yields

$$\begin{aligned} S_2^{\rm SE}(t, \tau=0, q_1, r_2, P_1, Y_2) &= C(0, q_1, r_2, P_1 + t\nabla_1 V_0, Y_2) - \frac{t}{2\Omega^2}(\nabla_2 V_0)^T \nabla_2 V_0 \\ &+ \frac{t}{4\Omega^2}\left(r_2^T \nabla_{22} V_0 r_2 + Y_2^T \nabla_{22} V_0 Y_2\right) \\ &- \frac{1}{\Omega^2}(\nabla_2 V_0(q_1 + tP_1, 0))^T Y_2, \end{aligned}$$

where the derivatives of V_0 are evaluated at $(q_1, 0)$ unless otherwise mentioned. We insert this expression in (97) and thus obtain

$$\begin{aligned} S_2^{\rm SE}(t,\tau,q_1,r_2,P_1,Y_2) &= C(0,q_1,r_2,P_1+t\nabla_1 V_0,Y_2) - \frac{t}{2\Omega^2}(\nabla_2 V_0)^T \nabla_2 V_0 \\ &+ \frac{t}{4\Omega^2}\left(r_2^T \nabla_{22} V_0 r_2 + Y_2^T \nabla_{22} V_0 Y_2\right) \\ &- \frac{1}{\Omega^2}(\nabla_2 V_0(q_1+tP_1,0))^T Y_2 \\ &+ \frac{1}{\Omega^2}(\nabla_2 V_0(q_1+tP_1,0))^T \left((\sin\tau) r_2 + (1-\cos\tau) Y_2\right). \end{aligned}$$

We now use the initial condition $S_2^{\rm SE}(t=\tau=0)=0$ to compute $C(t=0)$. We finally obtain

$$\begin{aligned} S_2^{\rm SE}(t,\tau,q_1,r_2,P_1,Y_2) &= \frac{1}{\Omega^2}(\nabla_2 V_0)^T Y_2 - \frac{t}{2\Omega^2}(\nabla_2 V_0)^T \nabla_2 V_0 \\ &+ \frac{t}{4\Omega^2}\left(r_2^T \nabla_{22} V_0 r_2 + Y_2^T \nabla_{22} V_0 Y_2\right) \\ &+ \frac{1}{\Omega^2}(\nabla_2 V_0(q_1+tP_1,0))^T \left((\sin\tau) r_2 - (\cos\tau) Y_2\right), \end{aligned} \quad (102)$$

with $\tau = t\Omega/\varepsilon$, where the derivatives of V_0 are evaluated at $(q_1, 0)$ unless otherwise mentioned. By construction, we have that $S_2(t) = S_2^{\rm SE}(t) + O(t^2)$.

Contents

Unité de recherche INRIA Rocquencourt
Domaine de Voluceau - Rocquencourt - BP 105 - 78153 Le Chesnay Cedex (France)

Unité de recherche INRIA Futurs : Parc Club Orsay Université - ZAC des Vignes
4, rue Jacques Monod - 91893 ORSAY Cedex (France)
Unité de recherche INRIA Lorraine : LORIA, Technopôle de Nancy-Brabois - Campus scientifique
615, rue du Jardin Botanique - BP 101 - 54602 Villers-lès-Nancy Cedex (France)
Unité de recherche INRIA Rennes : IRISA, Campus universitaire de Beaulieu - 35042 Rennes Cedex (France)
Unité de recherche INRIA Rhône-Alpes : 655, avenue de l'Europe - 38334 Montbonnot Saint-Ismier (France)
Unité de recherche INRIA Sophia Antipolis : 2004, route des Lucioles - BP 93 - 06902 Sophia Antipolis Cedex (France)

Éditeur
INRIA - Domaine de Voluceau - Rocquencourt, BP 105 - 78153 Le Chesnay Cedex (France)
http://www.inria.fr
ISSN 0249-6399